*Physics – Uspekhi* **38** (5) 521 – 543 (1995) 

PACS numbers: 87.22.Jb, 87.64.–t

# The physical bases of cell movement. The mechanisms of self-organisation of amoeboid motility

Yu M Romanovskii¶, V A Teplov

## Contents

**1. Introduction** **521**
**2. The basic phenomena of amoeboid motility** **522**
2.1 Characteristics of cell locomotion; 2.2 The mechanism of active contraction; 2.3 Two hypotheses of amoeboid movement
**3. Review of existing theories** **524**
3.1 Models for pseudopodium growth; 3.2 Interaction of cells with substrates; 3.3 Self-organisation of fountain flows in *Amoeba proteus*
**4. Autooscillations and biological motility** **527**
**5. Physarum polycephalum plasmodium as an autowave system** **528**
**6. Mathematical model for plasmodial autowave motility** **529**
6.1 Hydrodynamic equations for protoplasm motion in plasmodial strands; 6.2 Two-dimensional model of the plasmodium; 6.3 Equations for active stress and the controlling chain; 6.4 Linear analysis of equations of motion; 6.5 Quasi-harmonic autowaves; 6.6 Wave automodulation and quasi-stochastic regimes
**7. Physical methods for cell movement research** **535**
7.1 Cell tensiometry; 7.2 Laser Doppler anemometry; 7.3 Laser Doppler microscope
**8. Non-stationary external influences as a way of studying oscillatory motility** **538**
8.1 Synchronisation of shuttle protoplasmic movement by periodical changes of the temperature gradient; 8.2 The effect of light on plasmodium autowave regimes; 8.3 Mathematical model of a nonautonomous system
**9. Conclusion** **541**
**References** **541**

**Abstract.** Structure formation and autowave processes in active media far from equilibrium are the subject of a special division of the theory of nonlinear dynamic systems. In the present review the protoplasm of amoeboid cells is considered as an active medium, in which gel-like structures continuously assemble and disassemble. Local parts of these structures also spontaneously contract and relax, causing rather complex circular or shuttle-type flows of sol-like protoplasm. We consider several mathematical models of the resulting movements, wherein dissipative structures and the autowave processes mutually generate each other. The main quantitative features of the protoplasm dynamics in Physarum plasmodium are consistent with a model that postulates the existence of positive feedback between a local deformation and the free calcium level controlling the network contraction. The potentialities of different physical methods used to determine the values of parameters in the mathematical models are discussed.

¶This author's name is sometimes spelt Romanovsky in Western literature.

**Yu M Romanovskii** Faculty of Physics, Moscow State University, 119899 Moscow, Russia
E-mail: romanov@lbp.phys.msu.su
**V A Teplov** Institute of Theoretical and Experimental Biophysics, Russian Academy of Sciences, Pushchino, 142292 Moscow region, Russia
E-mail: teplov@venus.iteb.serpukhov.su

Received 23 January 1995
*Uspekhi Fizicheskikh Nauk* **165** (5) 555–578 (1995)
Supplied in English by the authors; edited by A Gelbtuch

## 1. Introduction

In recent years, owing to joint efforts of physicists, mathematicians, chemists, and biologists, autowave phenomena have become the most widely studied dynamic processes in open nonequilibrum distributed systems [1 – 6]. Nonlinear interactions between the variables of different nature evoke a loss of stability of stationary and uniform conditions when diffusion is taken into account. This results in the formation of strata in gaseous discharges, autosolitons in extended semiconducting and magnetic media, and a variety of flame propagation regimes [7 – 9]. The more complex the physical objects, the greater is the diversity of autowaves and self-organising structures. The autowave chemical reactions as well as numerous phenomena in neurodynamics are remarkable examples [10 – 12].

As will be shown below, the nonlinear physics of the self-organisation of protoplasm motility is also based on the laws of autowave processes. However, in addition to diffusion, hydrodynamic interaction via streaming protoplasm plays an appreciable role in the regulation of spontaneous intracellular contractions. In this regard the self-organisation of protoplasm motion combines features of active multiphase media where autowaves appear and

systems in which hydrodynamic instabilities arise. In the present review, using amoeboid cells as an example, we shall demonstrate how such intracellular self-movements are organised and what role they play in the mechanisms of cell migration.

The ability to move is one of the inalienable properties of all living things on the Earth. For Anton van Leeuwenhoek, who invented the microscope and was the first to observe cell movements, motility was synonymous with life: 'if it is alive it moves!' All the movements of which living systems are capable derive from motive activities within cells or groups of cells. On the cellular level motility is displayed in most diverse forms. It is not only the contraction of various types of muscle cells, resulting in animal locomotion, but also contractile activity of plant cells, producing, for example, the movement of mimosa leaves. These are also protoplasmic flows and various types of intracellular transport, playing an important role in the exchange and the distribution of substances within cells, individual movements of subcellular organelles, for example the periodic pulsation of the cell nucleus, the separation of chromosomes, division of a cell into two daughter ones, etc. Mechanical activity is also observed in neurons and is probably no less important than their electrical activity.

Motility is necessary both for free-living unicellular organisms to react to the environment (for example by avoiding toxic substances or, conversely, approaching food) and for tissue cells in multicellular organisms (for instance during embryogenesis). All these phenomena are based on the continuous process of self-organisation of locomotion and, in the case of amoeboid cells, also on the self-organisation of the motor apparatus itself. The cell is considered as an open nonequilibrum thermodynamic system, in which specialised structures form and collapse continuously and autowave movements arise.

There are three main mechanisms of cell locomotion, namely amoeboid, ciliary, and flagellar [13]. Amoeboid movement is the crawling of cells over a solid surface with the help of retractable extensions having the common name of pseudopodia (i.e. false feet). In contrast to pseudopodia, cilia and flagella are permanent special organelles allowing the cells to swim. In doing so bacteria use the rotating flagella whereas protista move in a liquid with the help of wavy beating of cilia or flagella. These various forms of locomotion have three common features. First, the great majority of cell movements is carried out by a few molecular motors transforming chemical energy into mechanical work. The working substances of these motors are pairs of specific macromolecules called contractile proteins. Three main pairs of the contractile proteins are known: actin–myosin used in muscles and amoeboid cells, and tubulin–dynein and tubulin–kinesin both working in ciliary motion and in the intracellular transport of organelles. Second, in all motile phenomena the coupled proteins are sliding past one another rather than contracting. And third, the energetic resources to keep these engines running are available as a result of direct conversion of chemical energy of adenosine triphosphate, ATP. Myosin, dynein, and kinesin are ATPases, i.e. enzymes ensuring ATP hydrolysis.

The emergence of contractile proteins appears to have beenoneofthemajorstepsintheevolutionofbiologicalcatalysis, the central role in which, in the opinion of Blyumenfel'd [14], should be given to slowly relaxing mechanical changes in enzymes. The structural and conformational reorganisations occurring in the contractile proteins are so pronounced that it is convenient to study the main principles of enzyme action using them as an example. Moreover, this fits neatly into the modern 'protein engine' concept [15]. Hence, it is quite probable that in living systems there is no physiological process in which the contractile proteins do not play an important role.

From the viewpoint of physics the protoplasm of an amoeboid cell is a truly unique object for the study of self-organisation in active distributed media. In this review we shall describe how dissipative structures and autowaves form in actomyosin solutions and which mechanisms does amoeboid motility involve. Gel-like structures continuously form and disappear as a result of assembly and breakup of the actomyosin network. The local regions of such networks can spontaneously contract and relax causing complex circular or back-and-forth flows of a sol-like protoplasm. The control of these processes is performed by changes of the system parameters and boundary conditions. Statement and solution of the problem on establishment of flow in a closed volume with an active actomyosin medium has some similarity with the problem of Benard convection in a viscous liquid layer heated from below. As we shall see, in the case of amoeboid movement, the concentration of the chemical regulator of contractile activity plays in some sense the role of the temperture gradient.

The peculiarity of self-organisation in an active actomyosin medium is the coexistence or, to be more exact, the mutual dependence of stationary spatial patterns or dissipative structures and self-sustained wave processes. Before dealing with the modern theory of these processes we shall discuss briefly the biophysical bases of actin–myosin interaction and amoeboid cell movement.

## 2. The basic phenomena of amoeboid motility

### 2.1 Characteristics of cell locomotion

Apart from proper amoebae many animal cells are capable under certain conditions of exhibiting the amoeboid motion. Hence, this type of movement is closely connected with a wide variety of important biological phenomena. In particular, it is involved in morphogenesis, i.e. structure formation during individual development, carcinogenesis, and immunity. The migrating cell represents a polar structure, at the front of which is an advancing pseudopodium. The central and rear parts of the cell are referred to as body and tail, respectively. At least two conditions must be met for a cell to move. First, the cell must be able to form pseudopodia the growth of which is accompanied by flow of the cell content into their space. Second, a solid substrate is required to which the pseudopodia could attach themselves. The shape of the pseudopodia and specific features of locomotion vary widely depending on the cell.

Lobopodia — wide blunt extensions — are characteristic of large fresh-water amoebae [16–18]. A region of clear ectoplasm free of granules, the so-called hyaline cap, is seen in their advancing part (Fig. 1). The inner granulated region of the cell containing the nucleus and other organelles is named the endoplasm. The endoplasm flows towards the front of an advancing pseudopodium and immediately behind the hyaline cap divides into lateral streams. This region, resembling a fountain, is called the fountain zone. In

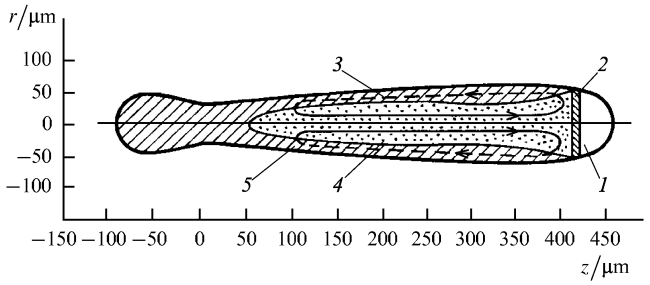


**Figure 1.** Schematic view of a medial cross-section of *Amoeba proteus* (adapted from Ref. [41]): (*1*) the hyaline cap, (*2*) the plasma gel sheet, (*3*) the gel-like ectoplasmic walls (shaded area), (*4*) the sol-like endoplasm, (*5*) the plasma membrane. The arrows show the direction of flow.

this zone the liquid endoplasm changes into gel-like ectoplasm, which forms new walls of the cell. In the hyaline cap there appear circular waves accompanied by pulsations of cap surface with the period of 10 s [18]. These pulsations are most probably connected with periodic detachments of thin layers of cortical gel from the membrane at the tip of the pseudopodium. Endoplasmic liquid squeezes through this plasma gel into the hyaline region and pushes the front edge of the membrane forward. Contractile proteins contained in the endoplasm serve as material from which a new gel layer is formed. Then the cycle is repeated and pulsatory progress of the cell continues.

Large amoebae that reach about 1 mm in linear size, such as *Amoeba proteus* (an amoeba capable of manifesting different forms) or Chaos-chaos (pay attention to the 'synergetic' sense of these old names!), can simultaneously extend several pseudopodia in different directions. These extentions compete among themselves and the ones that win are those which have sensed favorable gradients of chemical or physical factors: attractants, i.e. substances attracting a cell, humidity, light intensity, electric fields, etc. As the velocity of amoeba migration is about 1 μm $s^{-1}$ and that of protoplasmic flow is about 10 μm $s^{-1}$, these flows are easily detected under the microscope. In all cases of amoeboid locomotion the following chronological pattern of cell motile behaviour can be distinguished: the stage of pseudopodium protrusion, the stage of its distal attachment, and the stage of body contraction which causes detachment of the tail [13, 19].

In mammalian cells one can observe pseudopodia of another type; these are lamellopodia of various shapes. When cells of the connective tissue, the fibroblasts, spread, the lamella forms a ring of 1 μm or less in thickness arranged around the granular endoplasm [20–22]. The advance of the lamella in the course of spreading or migration is accompanied by ruffling. That is, local periodic protraction–retraction movements of the lamella edge result in the appearance of folds. This activity proceeds along the leading edge when the cell migrates, or around the whole perimeter when it spreads [21]. According to Refs [20, 23] the marginal region of the lamella should be considered as an excitable medium of spontaneously active elements. The dynamic competition of various lamella parts results in the polarisation of the cell which acquires a triangular shape. The fibroblast extends towards the active leading edge and the other parts of the lamella degenerate into a narrow tail zone. Sometimes circular propagation of contraction waves around the lamella perimeter is observed. Despite morphological variety the main physical mechanism is probably quite similar for all types of amoeboid movement.

As is clear from the above description the locomotion of amoeboid cells is a complex phenomenon dependent on coordinated interactions of many biochemical and biophysical processes. For its understanding it is necessary to solve two problems: how the forces for the extension of pseudopodia are generated and how mechanical and chemical processes are coordinated.

### 2.2 The mechanism of active contraction

Investigation of the mechanism of motility in living substances began from the study of striated muscles, in which the ability to contract is especially pronounced. Contractile proteins, actin and myosin, were first isolated from muscles. These proteins were later found to be present in the overwhelming majority of eukaryotic cells. Because of high structural regularity, the muscle is the best object for studying the mechanism of actin–myosin interaction [24, 25]. In contrast to striated muscles, which have permanent fibrils capable of unidirectional contraction and generation of large forces, the amoeboid cells generate force using a system of actin- and myosin-containing filaments able to assemble and to disassemble during the contraction process.

Actin in nonmuscle cells can exist in two functional states: as soluble monomers (G-actin) with a molecular mass of 42 kD, or in polymeric form as double-stranded filaments (F-actin) of various lengths. The double helix of F-actin has a diameter of 5–7 nm and a repeat step of 38 nm. In some actively moving cells actin can reach 20% –30% of the total protein content. A very critical factor for the polymerisation reaction which proceeds in the presence of ATP bound with monomers is the concentration of G-actin. The polymer that forms is always in equilibrium with the actin monomers in accordance with the following equation:

$$(\text{F-actin})_n \leftrightarrow (\text{F-actin})_{n-1} + (\text{G-actin}) ,$$

where $n$ is the number of chains in the polymer. Although the monomers can be added at either polymer end, one end is preferred for polymerisation and the other for depolymerisation. Actin molecules can interact with a number of so-called actin-binding proteins. Depending on the actin-binding protein, the patterns of actin arrangements can differ. Some proteins block its polymerisation, others bring about cross-linking of the actin filaments with each other or with other cell structures. This converts the microfilament suspension into a gel network, (Fig. 2) or, conversely, cuts the filaments onto short fragments leading to conversion of the gel into a sol. Myosin can also be related to the class of actin-binding proteins. It interacts only with the polymeric form of actin that produces motion.

Myosin is a hexamer composed of two heavy chains (with molecular mass of 200 kD each) and two pairs of light chains (with molecular mass of 16–22 kD each). The myosin heavy chains are highly asymmetric with a linear rod-like segment and a more globular head region. The rod parts of both heavy chains are coiled into a superhelix so that both heads appear at one end. Therefore the superhelix itself is called the tail. The tails of the myosin molecules can bind to each other and form various bipolar structures. In

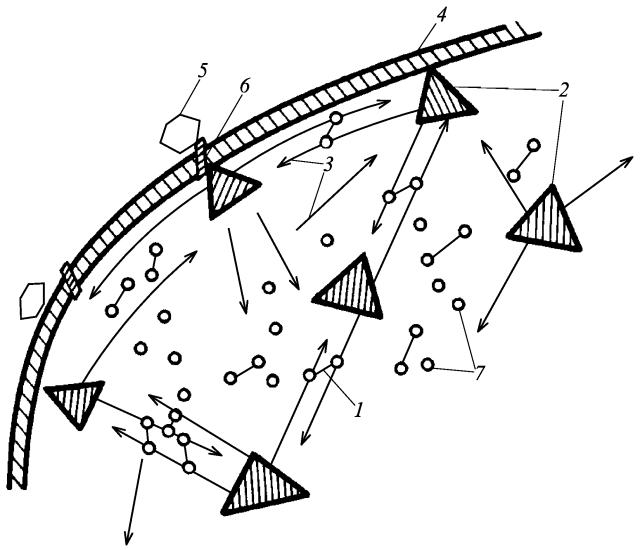


**Figure 2.** Schematic sketch of the actomyosin network (adapted from Ref. [31]): (*1*) myosin oligomers, (*2*) actin-binding nodes, (*3*) actin filaments formed as a result of G-actin polymerisation, (*4*) the plasma membrane, (*5*) adhesive proteins, (*6*) transmembrane proteins, (*7*) G-actin molecules.

nonmuscle cells myosin is able to form only small oligomers.

In view of similarity of the main contractile proteins of muscle and nonmuscle cells it can be assumed that the sliding mechanism observed in muscles operates in nonmuscle cells as well. In amoeboid cells, as a rule, one end of an actin filament is attached to the cell membrane (or to another cell organelle) and the other is free. Bipolar myosin oligomers are interposed between two opposing, and therefore oppositely polarised, actin filaments. In the process of interaction the actin filaments slide relative to myosin and the structures to which they are attached approach each other. Although the main components involved in the generation of driving forces are well known it is much less evident how the filament sliding is connected with the formation of pseudopodia and their activity.

### 2.3 Two hypotheses of amoeboid movement

As early as in the past century, long before the contractile proteins were discovered, various ideas on the mechanism of amoeboid movement had been put forward. Later they were revived in two main, but contradicting each other, theories of Mast [16] and Allen [17].

According to Mast's hypothesis, the movement of amoeba is due to continuous contraction of the ectoplasmic tube at the tail, which creates a pressure gradient along the cell body. The endoplasm is forced to flow towards the front with the resulting formation of pseudopodia. As ectoplasm contracts it solidifies, i.e. is converted into plasmasol. At the front the reverse process occurs: the endoplasm decreases its forward motion, spreads laterally, and gelates. Thus an ectoplasmic tube is continuously destroyed at the tail and rebuilt at the front. According to this concept the streaming of endoplasm and pseudopodium formation are passive events. This hypothesis dominated for nearly 40 years until a number of findings accumulated which it could not explain. First of all, a rather complex system is necessary to control positive taxis. So, attracting signals should be transmitted from the receptor sites at the front to the tail region. The tail contraction in turn would result in stretching all elastic regions rather then only the frontal zone.

The other idea, suggested by Allen [17], is known as the hypothesis of contraction in the fountain zone. Allen ascribed the active properties to the endoplasm, which according to him consists of an axial gel part and a more liquid peripheral part. Contractile force acts at the tip of advancing pseudopodium drawing the viscous endoplasm towards the front. Each portion of endoplasm advances towards the region of contraction, where it simultaneously contracts, gelates, and becomes inverted to form the ectoplasmic tube.

These two explanations are not theories, but rather concepts how an amoeba could move if only a certain portion of the cell were capable of force generation. However, the contractile proteins are omnipresent in the cell, so in order to solve the problem of amoeboid movement one should elucidate how these proteins are controlled. It is known that the interaction of actin and myosin is regulated by calcium ions. Certainly, other large and small molecules are also involved in their regulation. Nevertheless, the simplest theory of amoeboid motility and corresponding mathematical models may be constructed by considering only the spatiotemporal redistribution of $Ca^{2+}$ concentration which is an obligatory factor for self-organisation of intracellular movements.

## 3. Review of existing theories

The construction of a general quantitative theory of all events occurring in amoeboid cells is a complex and not yet completely resolved problem. However, there already exist a number of physical and mathematical models which describe the growth of pseudopodia [26–29], the processes of interactions of cells with the surface [30], and the organisation of intracellular movement [9, 31–33, 41, 82–85, 101]. In this section we shall first briefly review the theories of pseudopodium growth and then describe the problems of self-organisation of intracellular movements, which are, from our point of view, the most pithy and interesting for physicists. We will consider models for two characteristic cases, namely self-sustained fountain flows and autowave back and forth (shuttle) streaming of the protoplasm. In the general case these two forms of motility can coexist and govern the shift of the cell mass transfer and be, consequently, an integral part of the migration mechanism.

Important factors in the organisation of cell locomotion are gradients of various external stimuli including immune factors produced within multicellular organisms. It is just these effects, together with self-action of the cells through the substances which they secrete into external environment, that control the properties of the membrane and through it define the direction of migration [34]. Free-living cells also react with each other. Such collective phenomena are well expressed in the development of acrasiamycete *Dictyostelium discoideum* [9, 35] and in the behaviour of microorganisms when there is a deficit of food [36]. Therefore, a general model for cell migration should include a description of intracellular flows, the cell adhesion and detachment, the reception of external factors and, last, the biochemical procedure of signal transduction from

receptors to the contractile apparatus and to systems controlling membrane properties.

### 3.1 Models for pseudopodium growth

Several mathematical models for pseudopodium growth have been proposed. The processes of lamellipodium formation and pulling the cell forward are described in Refs [26–28]. It is assumed that local changes in ionic conditions caused by passive leakage through the leading membrane trigger the release of calcium ions which activate solating factors in the cytogel. These molecules sever some of the gel fibres, leading to partial degradation of the gel network. This reduces Young's modulus of the gel, allowing it to expand osmotically under the influence of its internal swelling pressure. This extends the leading edge of the lamella, which when it re-gels adheres to the substratum via adhesive sites. The calcium release also triggers the actomyosin gel to actively contract. However, little contractile stress can be generated until the calcium ions are resequestered by vesicles in the cytogel and the network reanneals. Then the gel contracts, and draws the cell ahead if the contraction is sufficient to break the posterior attachments to the substrate. Finally, the gel relaxes to its initial state, and the cycle reinitiates. Thus the ionic leak triggers a cycle of solation and swelling of the gel, followed by gelation and contraction. This cycle first spreads the lamella ahead of the cell, then pulls the cell up behind the advancing front.

A one-dimensional mathematical model is described in terms of the following field variables: $u(\boldsymbol{x},t)$ is the displacement of a material point in the gel from its initial position; $c(\boldsymbol{x},t)$ is the concentration of calcium ions; $G(\boldsymbol{x},t)$ is the volume fraction of the gel, i.e. the amount of actin that has been cross-linked into gel; $s(\boldsymbol{x},t)$ is the volume fraction of sol. This refers to all of the network subunits, including actin monomers and severed chain fragments, as well as the various actin-binding proteins. Unfortunately, Oster and Perelson [28] do not provide an analysis or numerical solutions of the derived equations.

Careful analysis of another mathematical model is presented in Ref. [29] devoted to the pseudopodium protrusion process in leucocytes. However, the central hypothesis of the theory seems to us to be open to question. In the proposed model, the pseudopodium is considered as a porous body made up of an F-actin network, the pores of which are full of aqueous solution. Actin monomers are considered as a 'solute' transported only by convection and diffusion in the liquid phase. The pseudopodium grows as actin filaments elongate at their ends at the tip of the pseudopodium. An essential concept in Ref. [29] is that the polymerisation of actin provides the energy for the advance of the front membrane of the pseudopodium and that the rate of growth of the pseudopodium is controlled only by actin-binding proteins. A one-dimensional moving boundary problem based on the proposed mechanism has been constructed and approximate solutions have been obtained. According to Ref. [29] this model is also applicable to the growth of other cellular systems such as extension of a long actin-filled tube known as the acrosomal process in sperm cells [37]. The acrosomal reaction is induced by contact of the sperm with the coat surrounding an egg. In sea cucumber sperm in less than 10 s the process can reach more than 90 μm in length — some 15 times as long as the head of the sperm. Through this tube the nucleus and cytoplasm of the sperm are drawn into the egg bringing about fertilisation.

There are a few other theoretical works concerned with this problem [38–40]. In our opinion the model proposed in Ref. [39] is more realistic. The authors have provided a detailed analysis of moving boundary models for extension of the acrosomal process and have estimated the kinetics of diffusion-limited actin polymerisation. It has been shown that actin filament growth occurs too slowly to drive acrosomal elongation and other forces, such as osmotically driven water flow through the membrane, must play an important role in causing the elongation. Actin polymerisation is a secondary phenomenon whose function is to impact an appropriate shape to the growing structure and stabilise it when the water flow ceases.

The works of Oster and co-authors [37, 38] suggest that the osmotic pressure arises from reactions at the membrane, which liberate osmotically active particles, and from the swelling of the actin gel attached to the membrane. The acrosomal process elongates under the action of the hydrostatic pressure gradient. The extension force is balanced by tension in the membrane and drag forces caused by the movement of the acrosomal membrane through the cell cytoplasm and through the external medium. During the acrosomal reaction new plasma membrane is inserted at the base of the acrosome and thus the membrane tension is probably negligible. In Refs [38, 40] the authors have numerically solved the corresponding equations and have shown that the solutions are in good agreement with available experimental data. In particular, it has been shown that the length of the model acrosome grows in proportion to the square root of time and the predicted rate of its extension quantitatively agrees with the real one.

### 3.2 Interaction of cells with substrates

In order to move forward the cell must exert a rearward force on its surrounding. It is therefore obvious that the mechanical and chemical properties of the environment will influence the rate of movement which greatly varies for different cells. For example, the speed of the fastest-moving white blood cells, neutrophil leucocytes, is about 30 μm $\text{min}^{-1}$, whereas that of fibroblasts is only 40 μm $\text{h}^{-1}$. Lymphocytes move slowly over planar substrates, but placed in a three-dimensional network matrix reach speeds comparable to those of neutrophil leucocytes.

Intuitively, three regimes of motile and adhesive behaviour can be envisaged for cell interaction with a substrate. On a poorly adhering surface a cell may stick so weakly that no traction is obtained and no net movement occurs. Alternatively, a cell may attach itself to a well-adhering surface so strongly that it becomes immobilised. With an optimum balance of adhesive forces, however, the cell may be mobile. The speed of cell migration in dependence on its adhesive properties has been estimated in Ref. [30]. The model proposed describes the cell cytoskeleton as a complex network of viscoelastic and contractile elements, relating intracellular forces to substratum traction forces mediated by adhesive-receptor bonds with substratum ligands. Net translocation of the cell requires an asymmetry in the cell–substratum interaction. Two alternative mechanism for generating such an asymmetry have been postulated: spatial distribution of cell surface adhesive receptors or spatial variation of their affinity with substratum. Numerical solution of the model equations has revealed the

influence of both mechanical properties of the cell and its adhesiveness to the substratum on the speed of motion that is in agreement with experimental data.

### 3.3 Self-organisation of fountain flows in *Amoeba proteus*

It is significant that there are protoplasmic streamings even when amoeboid cells are immobile. The following two modes of cytoplasmic motion can occur, preventing the mass from accumulating in the anterior part of the cell: either cyclic, reciprocal (shuttle) streaming or continuous, steady circular flow back and forth, usually in the form of axisymmetric fountain flow. The shuttle endoplasmic streamings are most clearly seen in *Physarum polycephalum* plasmodium, whereas fountain flows occur in the giant amoeba, *Amoeba proteus*.

Below, we will dwell on the theory of fountain flow in *Amoeba proteus* (Fig. 1). On the biological level a number of scenarios have been put forward, whereby fountain flows and the dynamic equilibrium between gel-like ectoplasm and sol-like endoplasm in the amoeba are maintained because of continuous association–dissociation processes in the actomyosin network as described above. In this section we shall briefly outline equations of the dynamics of such processes and basic results stemming from them. In our opinion the theory of fountain flows advanced by Dembo [41, 101] is most soundly based.

Following him, we shall regard the protoplasm as consisting of only two phases: actomyosin networks and an aqueous solution that fills the rest of the available volume. For simplicity, our consideration is restricted to models in which the network phase behaves as an isotropic viscous or pseudoplastic fluid. The following notation is used: $\rho$ is the volume fraction of the network phase; $V_j^{\mathrm{s}}$ and $V_j^{\mathrm{n}}$ are the velocity components of the solution and network phases, respectively. Then, in the Cartesian coordinate system, $(x_1, x_2, x_3)$, the rate-of-strain tensors for the network and solution phases will have the form:

$$E_{ij}^{\mathrm{n}} = \frac{\partial V_j^{\mathrm{n}}}{\partial x_i} + \frac{\partial V_i^{\mathrm{n}}}{\partial x_j}\,, \quad E_{ij}^{\mathrm{s}} = \frac{\partial V_j^{\mathrm{s}}}{\partial x_i} + \frac{\partial V_i^{\mathrm{s}}}{\partial x_j}\,, \quad i, j = 1, 2, 3\,. \tag{3.1}$$

The other functions in question will be the pressure of the solution phase, $P(x_1, x_2, x_3, t)$, and concentration of the chemical regulator of the contractile activity (say, calcium ions), $c(x_1, x_2, x_3, t)$. Taking into account that both the Reynolds number for the protoplasm motion and the volume fraction of the network are very much less than one, we obtain the following system of equations for the conservation of mass and momentum of the given biphasic medium:

$$\frac{\partial V_j^{\mathrm{s}}}{\partial x_j} = 0\,, \tag{3.2a}$$

$$\frac{\partial \rho}{\partial t} = -\frac{\partial}{\partial x_j}\left(\rho V_j^{\mathrm{n}}\right) + F\,, \tag{3.2b}$$

$$\frac{\partial}{\partial x_j}\left(\mu_{\mathrm{s}} M E_{ij}^{\mathrm{s}}\right) + \rho H\left(V_i^{\mathrm{n}} - V_i^{\mathrm{s}}\right) - \frac{\partial P}{\partial x_i} = 0\,, \tag{3.2c}$$

$$\frac{\partial}{\partial x_j}\left(\rho M E_{ij}^{\mathrm{n}}\right) + \rho H\left(V_i^{\mathrm{s}} - V_i^{\mathrm{n}}\right) - \frac{\partial}{\partial x_i}\left(\rho \Psi\right) = 0\,, \tag{3.2d}$$

$$\frac{\partial c}{\partial t} = -\frac{\partial}{\partial x_j}\left(c V_j^{\mathrm{s}}\right) + \frac{\partial}{\partial x_j}\left(\delta \frac{\partial c}{\partial x_j}\right) + S\,. \tag{3.2e}$$

Eqns (3.2b) and (3.2e) represent the balance conditions for the network density and the concentration of $Ca^{2+}$ ions, respectively, Eqn (3.2a) is the continuity equation for the solution phase, and Eqns (3.2c) and (3.2d) are the equations of motion for the solution and network phases, respectively. The analysis performed in Ref. [41] has led to the following expressions for the scalar functions $F$, $H$, $M$, $\Psi$, and $S$, which describe, respectively, the rate of network polymerisation (or depolymerisation); the specific hydraulic resistance of the network, used in Darcy's law for flow through a porous medium; the specific shear viscosity of the network, which depends on the number and strength of crosslinks between actin filaments; the specific contractile stress in the network; and the rate of increase (or decrease) of $Ca^{2+}$ concentration within the cytoplasm:

$$F = \frac{\rho_{\mathrm{e}} - \rho}{\tau_{\mathrm{n}}}\,, \quad H = \frac{\mu_{\mathrm{s}}}{m}\,, \quad M = \mu_{\mathrm{n}} \exp\left(\frac{\rho}{\rho_g}\right)^2\,,$$

$$\Psi = \Psi_0 (c - c_*)\,, \quad S = -\frac{c}{\tau_{\mathrm{c}}}\,. \tag{3.3}$$

Here the constant parameters $\rho_{\mathrm{e}}$ and $\tau_{\mathrm{n}}$ are the volume fraction of network at chemical equilibrium and the relaxation time of the polymerisation reaction, respectively. $\mu_{\mathrm{s}}$ is the solution viscosity, $m$ is the permeability coefficient, and $\mu_{\mathrm{n}}$ is the viscosity of the network. It has been assumed that contractile stress is a linear function of the calcium ion concentration with the proportionality constant $\Psi_0$. When calcium ion $Ca^{2+}$ concentration is above its threshold $c_*$, the active stress exceeds the swelling of the network. $\tau_{\mathrm{c}}$ denotes the characteristic lifetime of the calcium ions which are also capable of convection and diffusion in the solution phase with the diffusion constant $\delta$.

Numerical solutions of Eqns (3.2)–(3.3) have been obtained for cytoplasm contained in a fixed right circular cylinder whose boundary is divided into three natural surfaces: anterior, posterior, and lateral. Various variants of boundary conditions can be formulated by introducing $L_j$ and $N_j$, which are tangential and outward-normal components of a unit vector on the boundary surface. The solution and network phases are able to slip tangentially with respect to the plasma membrane; therefore 'slip' boundary conditions for the tangential velocity components are:

$$E_{ij}^{\mathrm{s}} N_i L_j = E_{ij}^{\mathrm{n}} N_i L_j = 0\,. \tag{3.4}$$

If the plasma membrane of the cell is impermeable to the flux of the solution phase, then the normal condition for the solution velocity is:

$$N_j V_j^{\mathrm{s}} = 0\,. \tag{3.5}$$

The normal boundary condition for the network velocity was taken to involve sticking to the posterior and lateral surfaces

$$N_j V_j^{\mathrm{n}} = 0\,, \tag{3.6}$$

and no sticking to on the anterior surface

$$E_{ij}^{\mathrm{n}} N_i N_j = -\frac{\Psi}{M}\,.$$

The last expression means that the network movement is subject to the constraint $N_i V^{\mathrm{n}} \leqslant 0$. Finally, simple Dirichlet boundary conditions for $Ca^{2+}$ ions on all boundary surfaces have been used:

$$c = \mathrm{const}\,. \tag{3.7}$$

The key result of Dembo's work is that he could find a real and self-consistent parameter combination of the

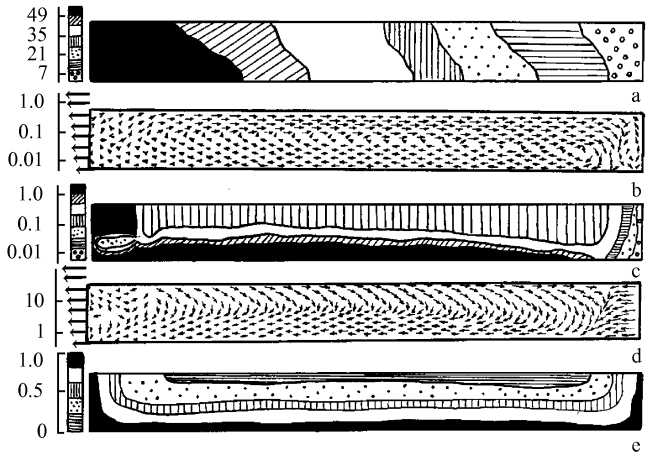


**Figure 3.** The results of computer simulation obtained by Dembo for his model of self-organising fountain flows in *Amoeba proteus* (adapted from Ref. [41]). Each subplot represents the lower half of a medial section through the cylindrical domain for which calculation has been per-formed. (a) The distribution of pressure, $P$ (dyn cm$^{-2}$); (b) the velocity field of solution phase, $V^s$ [μm s$^{-1}$]; (c) the distribution of network volume fraction, $\rho$ [dimensionless]; (d) the velocity field of network phase, $V^n$ [μm s$^{-1}$]; (e) the distribution of contractile activity regulator, $Ca^{2+}$ [dimensionless]. Corresponding scales are shown on the left of each subplot.

minimal model (3.2)–(3.3) which corresponded to experimental findings and most successfully described the self-organisation of the ectoplasmic wall, the hyaline cap, and the kinetics of fountain streaming. A low-resolution overview of the numerical solution of the minimal model obtained by Dembo is given in Fig. 3. Each map represents only the lower half of a medial section through the model amoeba. Appropriate scales are used to represent: (a) the distribution of the intracellular pressure, (b) the field of the phase velocities of solution, (c) the distribution of volume fraction of the network phase, (d) the field of its velocities, and (e) the distribution of the calcium ion concentration. One can see a rather sharp gradient of the network density separating ectoplasm and endoplasm. The ratio of values of $\rho$ in the ectoplasm and in the endoplasm amounting to 90%–95% also corresponds to experimental findings.

What is most important is the fact that, because of the boundary conditions at the anterior surface of the amoeba, the network phase is poorly anchored to the plasma membrane and forms a plasma gel sheet which impedes the flow of cytoplasmic granules into the hyaline area. This was the most difficult structure to explain theoretically. The other major result of the simulation is that it predicts a forward flow of both the solution and the network phases along the central axis and backward flow predominantly along the plasma membrane. According to the model the stationary pressure gradient, produced largely by contraction of the ectoplasmic tube, is established along the channel and drives a solution flow toward the anterior. The forward flow of the network is driven by the motion of the solution phase, but not vice versa as was hypothesised by Allen.

The distribution of calcium ions is seen to be diffuse throughout the length of the amoeba without a significant anterior–posterior gradient. The calcium concentration is maximum at the membrane and minimum at the centre. The final results are little affected by the exact form of positive $Ca^{2+}$ control on network contractility (linear or nonlinear). A stable steady state is established within 1 min starting from the completely uniform distribution (for comparison, the characteristic times are $\tau_c \sim 1$ s and $\tau_n \sim 10$ s).

The minimal model (Dembo's terminology) has made it possible to calculate the exact spatial distribution of both the power supplied by network contraction and the power lost as heat owing to internal viscosity and purely chemical processes, namely the hydrolysis of ATP during assembly and disassembly of the actomyosin network. The total rate at which the actomyosin network of one cell does mechanical work is $2.35 \times 10^{-5}$ erg s$^{-1}$. Of this amount $2 \times 10^{-5}$ erg s$^{-1}$ is converted to heat due to network viscosity, $0.34 \times 10^{-5}$ erg s$^{-1}$ is converted to heat by interphase drag, and a very small amount, about $0.005 \times 10^{-5}$ erg s$^{-1}$, is converted to heat by solution viscosity. About 35% of the power is derived from the small region at the very tip of the ectoplasmic tube, which is consistent with Allen's ideas. The heat liberated directly owing to chemical reactions occurring in the cell is much greater than the heat generated as a consequence of mechanical activity. For diverse cells, in general, the energy expended on maintaining the intracellular flows is significantly less than that required for other purposes [42].

As discussed earlier, there are cyclic waves of streaming associated with entrance of granular endoplasm into the hyaline cap region. Waves and hyaline cap cycles appear from their regularity to be autonomous oscillations. Dembo demonstrated that they can be simulated by his model with slightly different parameters. In the following, we will show that such regimes are normal in other amoeboid organisms [43, 82–85]. All details including numerical values of the model parameters and fine colour contour maps can be found in Refs [41, 101].

Although Dembo's minimal model successfully explains the main kinematic features of fountain streaming it has limitations which, in the first instance, stem from the fixed spatial domain. For amoeboid locomotion, movement of the cell boundary is of the essence. Elasticity of the actomyosin network and pressure gradient changes due to the ectoplasm deformation must also be taken into account. Below, we shall show that these factors are crucial for the initiation of shuttle endoplasmic flows in the plasmodium of another remarkable organism, myxomicete *Physarum polycephalum*.

## 4. Auto-oscillation and biological motility

One of interesting aspects of biological motility is its oscillatory nature. In this connection it should be mentioned that the majority of known cell oscillators have been found in cells with pronounced contractile activity. This may not only be due to the obviousness of these oscillations. A wide range of cellular processes can be involved in generating sustained oscillations [44]. It is usually supposed that such behaviour results from the instabilities that exist in metabolic or regulatory systems. This can result in a locally autonomous chemical oscillation forcing contraction and coupled in space by diffusion and convection. On this assumption, the mechanical organisation of the cell is not taken into consideration. However, it is know that many enzymes, for instance glycolytic ones, are tightly connected with a cytoskeleton, a deformation of which can change their activity. Turing in his classical work about morphogenesis

[45] already assumed that the chemical and mechanical processes in cells could influence each other.

The mechanical base of the cell, the cytoskeleton, is a complex macroscopic fibrous network attached to the plasma membrane. The major components of cytoskeleton are contractile proteins having ATPase activity, so the cytoskeleton can be considered to be an active distributed system. Since an enzymatic activity of the protein molecule depends on its conformation, a forced local deformation may change the enzymatic activity of the contractile proteins. This change may result in a change of their active tension which in turn results in deformation of the adjacent elements of the mechanochemical system and so on. Thus, this has an autowave character and is performed only by the mechanochemical system of the cell.

Mechanical stresses and strains can also change the conduction of ionic channels in the membranes of the cell and its organelles [46], which can result in spatio-temporal redistribution of the concentration of calcium ions. These findings suggest the existence of some feedback loops which could be sufficient to bring about auto-oscillations. If so, the cytoskeleton will be not only an effector system but an intrinsic part of the cell oscillator. Mechanical stresses affect the processes of self-organisation in multicellular organisms [47–50], in particular morphogenesis [9, 51]. Oscillators incorporating mechanical elements in feedback loops have the advantage of long-range hydrodynamic interactions, which is especially important for large systems with unexcitable membranes. In addition, in this case the oscillatory behaviour of a distributed mechanochemical system could be described by fewer differential equation.

## 5. *Physarum polycephalum* plasmodium as an autowave system

Unique opportunities for studying the problems of amoeboid motility, the physics of self-organisation, and mechanochemical auto-oscillations are provided by the *Physarum polycephalum* plasmodium. It is a multinuclear mass of protoplasm, surrounded by a common membrane and having an amoeboid type of motility. Because of its large size this huge cell has even been entered in the *Guinness Book of Records*. Growing on nutrient substrate the plasmodium looks like a sheet, the area of which can reach a square metre or more, and the thickness can attain 2 mm.

The motility of the plasmodium manifests itself as rhythmic pulsations of the plasmodial body and as vigorous reciprocating (shuttle) protoplasmic flows. Typically, their periods are in the range of 1–5 min. With the exhaustion of nutrients or with the appearance of gradients of various chemotactically active stimuli in a solid substratum, the plasmodium begins to migrate and in the process is organised into a fan-like front with a network of interconnected veins (so-called strands) at the back, which resemble blood vessels of the circulatory system (Fig. 4). The length of major strands can reach a few tens of centimetres and the diameter sometimes attains 2 mm. Within the strands and in channels throughout the frontal sheet, the protoplasm is differentiated into an outer tube-like gel ectoplasm and a more fluid inner sol endoplasm. Shuttle streaming is caused by nonstationary gradients of intracellular pressure generated by periodic contractions of actomyosin network in the ectoplasm.

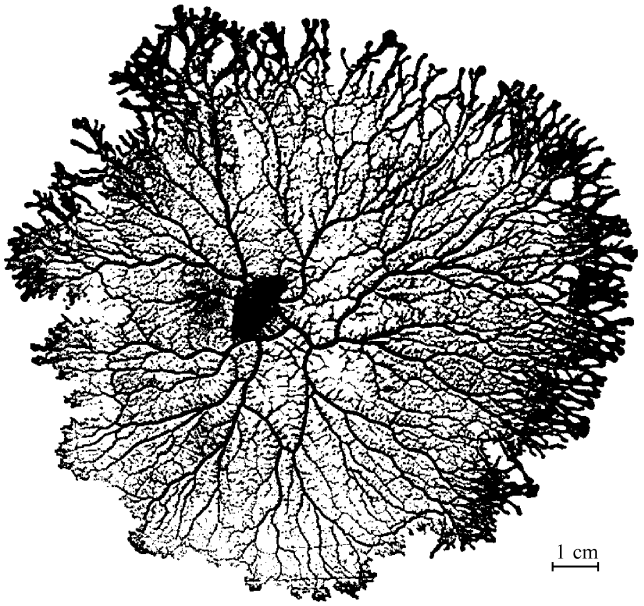


**Figure 4.** *Physarum polycephalum* plasmodium spreading over the substratum.

A great body of data on the plasmodial oscillatory activity has been obtained on isolated protoplasmic strands. A strand shows no significant rhythmic activity immediately after it has been excised from the mother plasmodium. Then, its injured ends are quickly regenerated and it begins to behave as an independent self-organising organism. Local regions of the strand begin to contract and relax, at first irregularly, but in 10–20 min their oscillations become synchronised and their amplitude increases. In time, the strand ends develop into frontal zones and a vigorous shuttle endoplasmic streaming is organised between them. So a quasi-standing wave of the fundamental tone arises. Later, one of the competing fronts becomes the leading front and the other degenerates leading to the characteristic polar form of migrating plasmodium [34, 52].

The pulsations of plasmodial body have a complex spatio-temporal organisation. In small plasmodia (5 cm or less in diameter) there are nearly synchronous and synphasic radial pulsations of all strands in the plasmodial network, contraction phases of the strands being coincident with the expansion phases of the advancing front [53]. Standing waves of higher harmonics can be set up in long isolated strands [54]. Propagation of peristaltic contractions has also been observed in such strands [55, 56]. Autowave motile activity of the plasmodium manifests itself most vividly in its frontal sheet. For example, quasi-stochastic oscillations of sheet thickness with their subsequent synchronisation and a wave-like propagation of loops with velocities of 5–30 $\mu m\ s^{-1}$ can be observed [54, 57]. Running waves can be induced artificially by the gradients of temperature or chemotactically active factors in the substratum [58]. Sometimes, in the frontal zone there is a circulation of such waves (circular or spiral waves).

Analysis of the wave processes requires a large number of simultaneous measurements in many points throughout the plasmodium. As a simple illustration, Fig. 5a shows a one-dimensional phase diagram of plasmodial thickness changes at twelve points at different instants. The diagram was constructed on the basis of movie pictures of a large

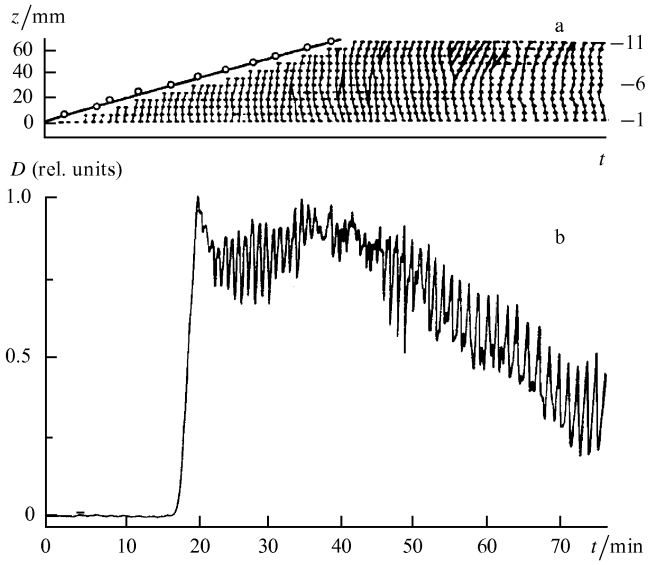


**Figure 5.** (a) Phase diagram of the contractile activity oscillation measured along the direction of plasmodial migration. Ordinate: position of the measurement point. Abscissa: current time. The dark bars parallel to the time axis represent the contraction phase and the gaps show relaxation phases. (b) Oscillations of the plasmodium thickness obtained for the 6th point of measurement. Ordinate: relative optical density. Abscissa: current time.

plasmodium, migrating on nonnutritive agar gel along a narrow track bordered by non-adhesive paraffin strips. A typical record of changes in the image optical density is shown in Fig. 5b. Inclinations of the continuous lines connecting the points of the same contraction phases determine phasic wave velocities which depend on the plasmodium size. In the given case these velocities reach 2 cm $s^{-1}$, that is much more than the average velocity of the front which is here equal to 8 cm $h^{-1}$.

In parallel with the contractile oscillations in the plasmodium there also occur simultaneous and synchronous oscillations of the membrane potential, of the concentrations of $Ca^{2+}$ [59, 60], $H^+$ [61], ATP [62], etc. The question arises whether or not there is a common mechanism underlying all such oscillatory behaviour, i.e. is it possible to isolate those processes directly responsible for generating the rhythm. The important feature of electrical and chemical oscillations observed in *Physarum* is that they are always accompanied by mechanical oscillations but not vice versa. This might reflect participation of the cytoskeleton in the feedback loops responsible for auto-oscillations.

One of the striking characteristics of plasmodial strands, suggesting the existence of some feedback loop which can be sufficient for causing auto-oscillations, is their strain-induced activation. When a strand under isometric conditions is quickly stretched by 10% – 20% of its length, the tension and the amplitude of its oscillations conspicuously increase. Under isotonic conditions, the increase in the load gives rise to an increase in the amplitude of length oscillations, which is also proportional to the tension [63, 64].

Eruptions of the endoplasm after strand punctures indirectly indicate the existence of hydrostatic pressure and hence of tension in the ectoplasm attached to the plasma membrane. As the cell membranes are well permeable to water, osmotic forces should come into play in the maintenance of intracellular pressure. The complex of cytoskeleton and plasma membrane in the broad sense is a unitary system capable of storing a great deal of mechanical energy. The elasto-osmotic parameters of the plasmodium have been estimated by Lairand et al. [65, 66]. In particular, for plasmodia adapted to water, the osmotically active concentration was shown to average 70 mos M. The osmotic pressure corresponding to this value is equal to $1.7\times10^6$ dyn $cm^{-2}$. A marked decrease in the elasticity and viscosity of the strands, observed after their treatment with strong attractants, causes a drop in the intracellular pressure along with a decrease in both the amplitude and the period of motive force oscillations [67 – 69]. Data obtained in these experiments give a lower estimate for the intraplasmodial pressure value as about $10^4$ dyn $cm^{-2}$.

If the reception of attractants results in a local relaxation of the ectoplasm, the existence of turgor pressure could explain the directed endoplasmic flow into forming pseudopodium and essentially simplify the problem of how cell migration is controlled. In this event the cell orientation will occur not because of local active contraction, as Mast's and Allen's models postulate, but because of maintenance of global cell tones and a local decrease of elasticity in the place where the new front should form. The latter can be caused by attractant binding to receptor and subsequent activation of actin-modulating proteins.

The essential role of the plasmodial cytoskeleton in the observed autowave phenomena is also indicated by data on the synchronisation of auto-oscillations throughout the plasmodium. The synchronisation is not connected with electrical phenomena, as it does in excitable tissues [70, 71]. The necessary condition for synchronisation has been shown to be the pressure of shuttle endoplasmic streaming [72 – 75]. This key circumstance should be taken into account in the mathematical modeling of autowave motility in the *Physarum* plasmodium.

## 6. Mathematical model for plasmodial autowave motility

### 6.1 Hydrodynamic equations for protoplasm motion in plasmodial strands

Mathematical models for shuttle streaming in isolated plasmodial strands were first proposed for a dumbbell-shaped fragment [76 – 78]. These discrete models describe the movements of viscous liquid between two volumes coupled by a rigid tube. Here we consider one- and two-dimensional distributed models, which are considerably closer to real objects, that is an isolated long plasmodial strand [79 – 83] and a plasmodial sheet [84] (a form characteristic of early stages of plasmodium spreading). In all cases the longitudinal deformation of ectoplasm is assumed to be impossible because of strong adhesion of the cell to the underlying substratum.

The protoplasmic strand is considered as a long cylindrical tube filled with an incompressible endoplasm. Actomyosin fibrils are homogeneously distributed in the ectoplasmic wall and attached to the membrane. The interaction of actin and myosin can be regulated by many factors, but for simplicity we shall consider only calcium ions. It is assumed that there is a sufficient local supply of ATP. A spontaneous increase in $Ca^{2+}$ ion

concentration in some section of the strand causes a local ectoplasm contraction. This leads to a decrease in strand diameter and pumping of endoplasm into the neighbouring regions. Stretching the ectoplasmic walls in these parts of the strand is assumed here to promote an increase in $Ca^{2+}$ ion concentration. In this way conditions for a new active contraction are created, but now in the sections adjacent to the original contraction, and so on. Under certain boundary conditions this autowave process can results in travelling or standing waves of radial ectoplasm contractions and in periodic flows of endoplasm. To elucidate this possibility it is necessary to express the above description in mathematical terms.

Let us consider nonstationary axisymmetric flow of an incompressible viscous (in the first approximation Newtonian) fluid in a long cylindrical tube with a viscoelastic impermeable active wall (Fig. 6a). As the Reynolds number for this case is very small ($\mathrm{Re} \sim 10^{-6}$), the endoplasm streaming may be described by the equation for Poiseuille flow in a tube with a gently varying radius:

$$\frac{\partial P}{\partial z} = -\frac{8\mu}{R^2} V \,. \tag{6.1}$$

Here $V(z, t)$ is the velocity of endoplasm averaged over the cross section of the strand lumen, $P(z, t)$ is the intracellular pressure, $\mu$ is the endoplasm viscosity, and $R$ is the mean radius of the strand.

To find the relationship between $V(z, t)$ and small deviations, $x(z, t)$, of the radius from its mean value ($x \ll R$) we write down the continuity equation:

$$\frac{\partial v_z}{\partial z} + \frac{1}{r}\frac{\partial}{\partial r}(r v_r) = 0 \,, \tag{6.2}$$

where $v_z$ and $v_r$ are the longitudinal and radial components of endoplasm velocity, respectively. Integrating this equation over the cross-sectional area of the strand lumen and taking into account the fact that typical lengths of autowaves observed in the plasmodium are much greater than its characteristic thickness, $\lambda^* \gg R$, we obtain:

$$\frac{\partial V}{\partial z} = -\frac{2}{R} v_r\Big|_{r=R} = -\frac{2}{R}\frac{\partial x}{\partial t} \,, \tag{6.3}$$

where

$$V(z, t) = \frac{1}{\pi R^2}\int_0^R 2\pi r v_z \, \mathrm{d}r \,.$$

Differentiating Eqn (6.1) with respect to $z$ and introducing expression (6.3) we obtain:

$$\frac{\partial^2 P}{\partial z^2} = \frac{16\mu}{R^2}\frac{\partial x}{\partial t} \,. \tag{6.4}$$

Further, neglecting the radial inertial forces acting on the wall element and nonuniformity in the distribution of stresses and strains across the wall thickness we find the expression connecting $x(z, t)$ with the active component of the intracellular pressure. Rheological properties of the wall will be described on the basis of the analog model scheme in Fig. 12. Experimental justification for choosing this scheme is given below in Section 7. The behaviour of this scheme is described by the following equation connecting the total tangential stress averaged across the wall thickness, $\sigma$, with the active stress, $\sigma_A$, generated by actomyosin interactions and the passive stress, $\sigma_p$, dependent on relative deformations, $\varepsilon$, of the elastic ($E_1$, $E_2$) and viscous ($\eta$) elements:

$$\tau_1 \frac{\partial \sigma}{\partial t} + \sigma = E_1\left(\tau_2 \frac{\partial \varepsilon}{\partial t} + \varepsilon\right) + \tau_1 \frac{\partial \sigma_A}{\partial t} + \sigma_A \,, \tag{6.5}$$

where $\tau_1 = \eta/E_2$ and $\tau_2 = \eta(1/E_1 + 1/E_2)$ are the characteristic relaxation times.

When the ratio of the wall thickness, $h$, to the strand radius is small, then $x(z, t) = R\varepsilon(z, t)$ and the intracellular pressure and its active component are equal to $P(z, t) = \sigma(z, t)h/R$ and $P_A(z, t) = \sigma_A(z, t)h/R$, respectively. Taking this into account we differentiate Eqn (6.5) twice with respect to $z$ and introducing expression (6.4) we obtain an equation governing radial contraction of the strand:

$$\frac{16\mu\tau_1}{R^3}\frac{\partial^2 x}{\partial t^2} + \frac{16\mu}{R^3}\frac{\partial x}{\partial t} = \frac{E_1 h\tau_2}{R^2}\frac{\partial^3 x}{\partial t\,\partial z^2} + \tau_1\frac{\partial^3 P_A}{\partial t\,\partial z^2} + \frac{E_1 h}{R^2}\frac{\partial^2 x}{\partial z^2} + \frac{\partial^2 P_A}{\partial z^2} \,. \tag{6.6}$$

The order of this equation is reduced if $\tau_1 = 0$ (or $E_2 \to \infty$), i.e. if the passive viscoelastic properties of the wall are represented by the Kelvin rheological model. In this case an expression for intracellular pressure in dependence on the wall parameters is of the simple form [85]:

$$P(z, t) = \frac{E_1 h}{R^2} x + \frac{\eta h}{R^2}\frac{\partial x}{\partial t} + P_A(z, t) \,. \tag{6.7}$$

Accordingly, within this approximation, Eqn (6.6) becomes:

$$\frac{16\mu}{R^3}\frac{\partial x}{\partial t} = \frac{\eta h}{R^2}\frac{\partial^3 x}{\partial t\,\partial z^2} + \frac{E_1 h}{R^2}\frac{\partial^2 x}{\partial z^2} + \frac{\partial^2 P_A}{\partial z^2} \,. \tag{6.8}$$

Eqns (6.6) and (6.8) can be complemented by terms allowing for viscoelastic forces exerted along the strand wall which is attached to the underlying substratum and is in tension. This gives rise to an additional passive pressure in expression (6.7). For small, radially symmetrical deforma-

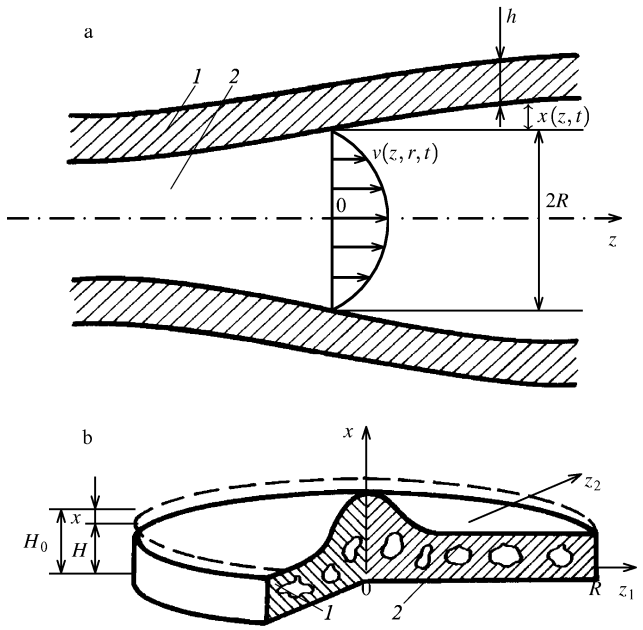


**Figure 6.** Schematic sketch of a protoplasmic strand (a), and of the whole plasmodium at the early stage of spreading (b): (*1*) the ectoplasm, (*2*) the endoplasm.

tions of the strand it can be written as the following approximation:

$$P'(z, t) = \frac{E'I}{2\pi R}\frac{\partial^4 x}{\partial z^4} + \frac{\eta' I}{2\pi R}\frac{\partial^5 x}{\partial t\,\partial z^4} + \frac{\sigma'}{2\pi R}\frac{\partial^2 x}{\partial z^2} . \qquad (6.9)$$

Here $E'$ and $\eta'$ are Young's modulus and viscosity coefficient of the wall for longitudinal deformations, respectively, $I = \pi R h^3/6$ is the moment of inertia of the wall section, $\sigma' = 2\pi R h E' \varepsilon'$ is the longitudinal tension of the strand, where $\varepsilon'$ is the longitudinal deformation of the wall. Since $\varepsilon'$ can reach 0.1 in practice, the last term in expression (6.9) is of primary importance.

We shall restrict our consideration to the conditions corresponding to fixed plasmodial boundaries. In the case of isolated strand fragments of constant length, $L$, and with closed boundaries it follows that:

$$V\Big|_{z=0,\,L} = \frac{\partial P}{\partial z}\Big|_{z=0,\,L} = 0 . \qquad (6.10)$$

This expression in combination with Eqn (6.7) allows us to write the boundary conditions as:

$$\left(\frac{\partial P_A}{\partial z} + \frac{E_1 h}{R^2}\frac{\partial x}{\partial z} + \frac{\eta h}{R^2}\frac{\partial^2 x}{\partial z\,\partial t}\right)\Big|_{z=0,\,L} = 0 . \qquad (6.11)$$

The following simplified boundary conditions [85] can also be used:

$$\frac{\partial x}{\partial z}\Big|_{z=0,\,L} = 0 ; \qquad (6.12)$$

this corresponds to the experimental finding that the standing wave along the strand is cosine-shaped with antinodes at the ends of the strand. In the case of a circular strand of length $L$, the boundary conditions are:

$$x|_{z=0} = x|_{z=L}, \qquad \frac{\partial x}{\partial z}\Big|_{z=0} = \frac{\partial x}{\partial z}\Big|_{z=L} . \qquad (6.13)$$

### 6.2 Two-dimensional model of the plasmodium

Plasmodium spreading on a surface can be represented as a viscoelastic porous round plate whose diameter is much greater then its thickness (Fig. 6b) [84]. The pores — stochastically distributed channels in which the endoplasm streams — form within the ectoplasmic gel containing actomyosin.

Flows through porous medium are described by Darcy's law:

$$\boldsymbol{V} = \frac{mH^2}{\mu}\nabla P . \qquad (6.14)$$

Here $\boldsymbol{V}(t, z_1, z_2)$ is the horizontal endoplasm velocity averaged over the vertical coordinate $x$, $P(t, z_1, z_2)$ is the intracellular pressure, $H(t, z_1, z_2)$ is the plate thickness, $m = \text{const} > 0$ is the porosity coefficient equal to the ratio of pore volume to plate volume, $\mu$ is the endoplasm viscosity. Further, using the same line of reasoning as for deriving the equations for the strand we can obtain in the Kelvin approximation an equation for a plasmodium in the shape of a two-dimensional thin plate:

$$\frac{\partial x}{\partial t} = \frac{H_0^2 m}{\mu}\left(E\Delta x + \eta\Delta\frac{\partial x}{\partial t}\right) + \frac{H_0^3 m}{\mu}\Delta P_A , \qquad (6.15)$$

Here $x(t, z_1, z_2) = H_0 - H(t, z_1, z_2)$, $H_0 = \text{const} > 0$ is the plasmodium film thickness in the absence of stresses. The boundary conditions for the two-dimensional case are:

$$\left(\nabla P_A + \frac{E}{H_0}\nabla x + \frac{\eta}{H_0}\nabla\frac{\partial x}{\partial t}\right)\Big|_{\Im} = 0 \qquad (6.16)$$

Where $\Im$ is the outer boundary of the plasmodial sheet.

### 6.3 Equations for the active stress and the controlling chain

Since the main contractile proteins of plasmodium and muscles are very similar, it can be assumed that the qualitative features of their biochemical behaviour are very much alike and that the mechanochemical cycle in the plasmodium also consists of many elementary stages of interaction of actin and myosin with low-molecular-mass components and with each other [24, 25, 85]. Fig. 7 shows a simplified scheme where only two mechanically important states of myosin oligomers (dimers) are considered, namely the free state (detached dimers) and the bound state (myosin heads attached to two oppositely polarised actin filaments). When new ATP molecules are hydrolysed, this cycle is repeated over and over again, and when myosin oligomers are abundant in fibrillar space, the sliding of actin filaments becomes macroscopic. Such a mechanochemical cycle can be represented as follows:

$$A + M \underset{k_2}{\overset{k_1'}{\rightleftarrows}} N .$$

The corresponding kinetic equation will then have the form:

$$\frac{\partial n}{\partial t} = k_1' a m - k_2 n , \qquad (6.17)$$

where $k_1'$ and $k_2$ denote the effective rate constants for the formation and dissociation of actomyosin complexes, respectively. $a(z, t)$, $m(z, t)$, and $n(z, t)$ are the numbers of myosin-binding centres on actin filaments ($A$), and of free ($M$) and bound ($N$) myosin dimers, respectively. Obviously $a = a_0 - n$, $m = m_0 - n$, where $a_0$ and $m_0$ are the total numbers of $A$ and $M$, respectively. It is known that for the *Physarum* plasmodium $a_0 \gg m_0$ [86]; hence one may assume $a \approx a_0$. As distinct from the theory of muscle contraction [24], inhibiting cross-bridges are ignored in this simplified consideration; the active stress $\sigma_A$ will then be

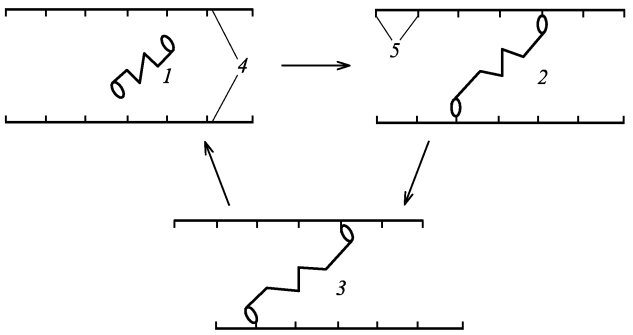


**Figure 7.** A simplified representation of the mechanochemical cycle in the *Physarum* plasmodium: (*1*) the free myosin dimer, (*2*), (*3*) the dimers attached to the actin filaments, (*4*) the actin filaments, (*5*) the myosin-binding centres of the actin filaments.

proportional to $n$, and the following equation for the tangential active stress can be obtained from Eqn (6.17):

$$\frac{\partial \sigma_A}{\partial t} = k_1(\sigma_0 - \sigma_A) - k_2\sigma_A \ , \tag{6.18}$$

where $k_1 = k_1' a_0$, and $\sigma_0$ is the maximum active stress which occurs when all myosin oligomers participate simultaneously in force generation.

It is now well established that the rhythmic contractions in the *Physarum* plasmodium are accompanied by synchronous oscillations of calcium ion concentration [59, 60]. Calcium control of the actin–myosin interaction can be ensured by making the rate constant $k_1$ in Eqn (6.18) dependent on $Ca^{2+}$ ion concentration. It is known that the dependence of contractile activity in plasmodial strands on free calcium concentration has a threshold character [87, 88]. Yoshimoto and Kamiya [88] observed that the active stationary tension of the strand starts to increase at the $Ca^{2+}$ concentration of $c_1 = 6 \times 10^{-8}$ M and reaches maximum at $c_2 = 10^{-7}$ M. Therefore, we can represent $k_1$ as a function:

$$k_1 = k_1 f(c) \ , \tag{6.19}$$

where $c$ denotes the $Ca^{2+}$ concentration. The appearance of the dimensionless function of activation $f(c)$ is shown in Fig. 8. Taking account of expression (6.19) we can rewrite Eqn (6.18) for thin-wall strands as:

$$\frac{\partial P_A}{\partial t} = k_1 f(c)\,(P_0 - P_A) - k_2 P_A \ , \tag{6.20}$$

where $P_0 = \sigma_0 h/R$ is the maximum active component of intracellular pressure.

The simplest equation coupling mechanical strain and calcium homeostasis (feedback loop equation) is:

$$\frac{\partial c}{\partial t} = k_3 x(c_0 - c) - k_4 c \ . \tag{6.21}$$

Here $c_0$ is the maximum $Ca^{2+}$ concentration for the case when all calcium ions are released from their storages. It is assumed that the rate of $Ca^{2+}$ inflow into the fibrillar space increases linearly with $x$, and that sequestration of calcium ions into the storages obeys first-order kinetics. For simplicity, we have not taken into account diffusion and drift of $Ca^{2+}$ ions with endoplasmic streaming and confined ourselves to elucidating the possibility of only hydrodynamic interaction between different sections of the strand. As the concentration of calcium ions oscillates within a narrow interval $c_1 < c < c_2$ (see Fig. 8), Eqn (6.21) can be simplified:

$$\frac{\partial c}{\partial t} = k_3 x - k_4 c \ . \tag{6.22}$$

It should be noted that more complex models for calcium regulation [76, 77] have been proposed. In these models, in addition to control via mechanical strain, calcium-induced $Ca^{2+}$ release and the drift of calcium ions with endoplasmic flow are considered. Recently calcium ion oscillations have been modeled purely on the basis of biochemical reactions. From our viewpoint the replacement of Eqn (6.21) by a system of kinetic equations for biochemical reactions is quite possible. But whatever the model the influence of mechanical stresses on these reactions taken into account.

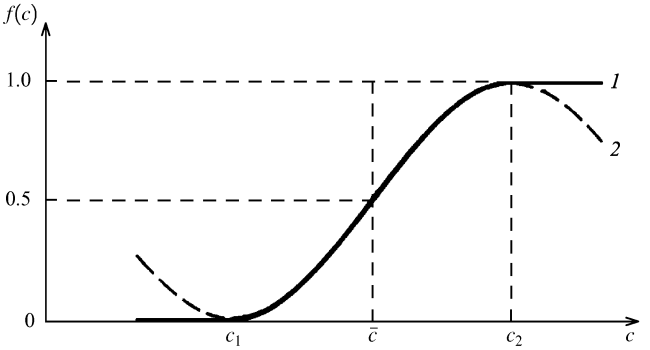


**Figure 8.** Activation function, $f(c)$, (curve *1*) and its approximation at $c_1 \leqslant c \leqslant c_2$ by a polynomial of the third degree (curve *2*).

## 6.4 Linear analysis of equations of motion

To summarise briefly, basic equations (6.6) [or (6.8)], (6.20), (6.21) [or (6.22)] with boundary conditions (6.11), (6.12) [or (6.13)] describe the distributed auto-oscillations of $x$, $P_A$, and $c$ in the long fragment of (or circular) strand, whereas basic equations (6.15), (6.20), (6.21) [or (6.22)] with boundary conditions (6.16) describe those in the spreading plasmodium.

The mathematical problems connected with proofs of the existence and uniqueness of the solution of the system of equations are considered by Pavlov and Potapov [90, 91], where the authors also extend the equations given above to the case where the coefficients are functions of the coordinates and time. All this has allowed us to obtain a number of interesting results adequately explaining biological properties of the *Physarum polycephalum* plasmodium.

Some of the approximate solutions of the basic system of equations have been obtained in the following manner [82–85]:

1. Steady state (stationary) solutions $\bar{x}$, $\bar{P}_A$, $\bar{c}$ for both the one-dimensional strand and the two-dimensional plasmodial sheet have been found. They are defined by the following system of nonlinear algebraic equations:

$$\begin{aligned} &\frac{Eh}{R^2}\,\bar{x} + \bar{P}_A = P_r \ , \\ &k_1 f(\bar{c})\,P_0 - \left(k_1 f(\bar{c}) + k_2\right)\bar{P}_A = 0 \ , \\ &k_3\bar{x} - k_4\bar{c} = 0 \ . \end{aligned} \tag{6.23}$$

Here $P_r$ is an integration parameter defining an intracellular hydrostatic pressure which at the given boundary conditions does not depend on $z$. The necessary condition for the existence of a hydrostatic pressure in the cell is an osmotic inequality between the surrounding fluid and the interior of the cell [65, 66].

The cell adjusting its water content can change $P_r$ and consequently $\bar{x}$, $\bar{P}_A$, $\bar{c}$. In radiophysical terms, the cell chooses a working point on the characteristic function $f(c)$ (Fig. 8). When $f(c)$ is a monotonously increasing function and $P_r$ is constant then Eqns (6.23) have a unique and spatially uniform solution, that is, $\bar{x}$, $\bar{P}_A$, $\bar{c}$ are real constants.

2. The stability of the stationary solution of the linearised system has been investigated. Small wave-like perturbations have been introduced:

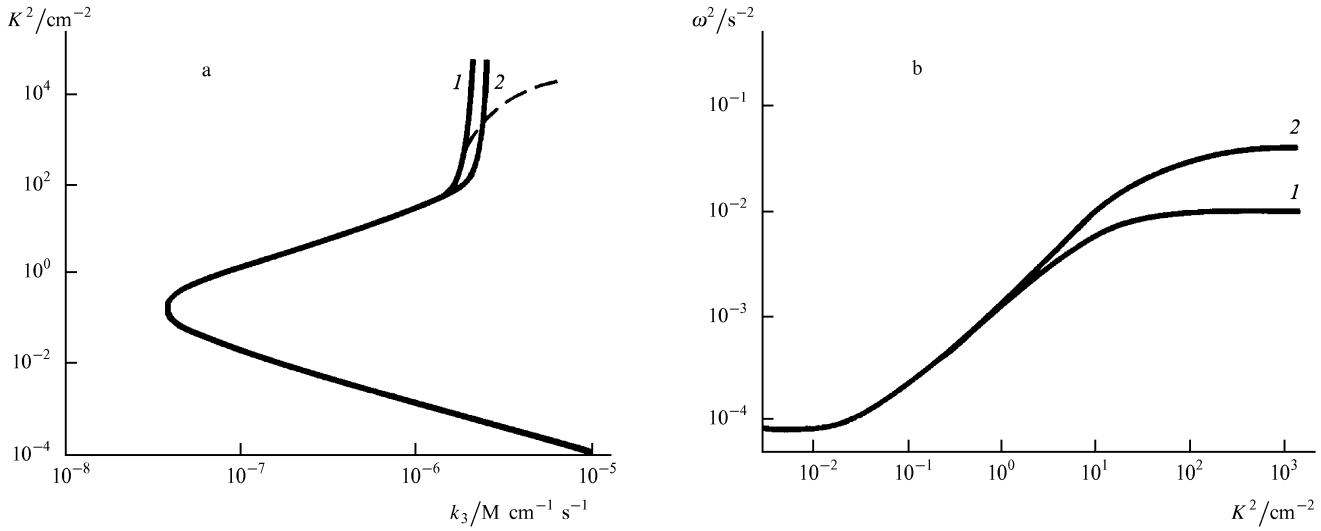


**Figure 9.** (a) The boundaries of the loss-of-stability regions for models of the fourth (*1*) and the third (*2*) order. The square of the wave number, $K^2$, is plotted against the parameter of positive feedback, $k_3$. Self-excitation conditions of autowaves are fulfilled to the right. The dashed curve shows the upper limit for the wave number when Eqn (6.9) is taken into account. (b) Dependence of the square of the frequency, $\omega^2$, on $K^2$, corresponding to the boundaries of stability loss shown by curves *1* and *2* in (a).

$$\begin{bmatrix} x \\ P_A \\ c \end{bmatrix} = \begin{bmatrix} \bar{x} \\ \bar{P}_A \\ \bar{c} \end{bmatrix} + \begin{bmatrix} \alpha \\ \beta \\ \gamma \end{bmatrix} \exp(pt)\cos(Kz)$$

for the strand, and

$$\begin{bmatrix} x \\ P_A \\ c \end{bmatrix} = \begin{bmatrix} \bar{x} \\ \bar{P}_A \\ \bar{c} \end{bmatrix} + \begin{bmatrix} \alpha \\ \beta \\ \gamma \end{bmatrix} \exp(pt)\cos(K_1 z_1)\cos(K_2 z_2)$$

for the sheet. In the latter case cylindrical coordinates can also be used. Here $\alpha \ll \bar{x}$, $\beta \ll \bar{P}_A$, $\gamma \ll \bar{c}$. Then, the dispersion equation coupling the complex frequency, $p$, and the square of the wave number, $K^2 = K_1^2 + K_2^2$, can be written as:

$$a_0 p^4 + a_1 p^3 + a_2 p^2 + a_3 p + a_4 = 0\,, \tag{6.24}$$

where

$$a_0 = \frac{16\mu}{R}\tau_1\,,$$

$$a_1 = \eta h K^2 + \frac{16\mu}{R}\left\{1 + \tau_1\left[k_1 f(\bar{c}) + k_2 + k_4\right]\right\},$$

$$a_2 = \left\{E_1 h + \eta h\left[k_1 f(\bar{c}) + k_2 + k_4\right]\right\}K^2 + \frac{16\mu}{R}\left\{k_1 f(\bar{c}) + k_2 + k_4 + \tau_1 k_4\left[k_1 f(\bar{c}) + k_2\right]\right\},$$

$$a_3 = \left\{E_1 h\left[k_1 f(\bar{c}) + k_2 + k_4\right] + \eta h k_4\left[k_1 f(\bar{c}) + k_2\right] + \tau_1 \frac{k_1 k_2 k_3 f'(\bar{c})}{k_1 f(\bar{c}) + k_2} R^2 P_0\right\}K^2 + \frac{16\mu}{R} k_4\left[k_1 f(\bar{c}) + k_2\right],$$

$$a_4 = \left\{E_1 h k_4\left[k_1 f(\bar{c}) + k_2\right] + \frac{k_1 k_2 k_3 f'(\bar{c})}{k_1 f(\bar{c}) + k_2} R^2 P_0\right\}K^2\,.$$

Analysis of this equation as well as of the dispersion equation of a lower order corresponding to the Kelvin approximation ($\tau_1 = 0$) has shown that in such systems, in accordance with the Routh–Hurwitz criterion, only an oscillatory instability is possible and the condition for self-excitation is given by:

$$a_1 a_2 a_3 - a_0 a_3^2 - a_1^2 a_4 \leqslant 0\,. \tag{6.25}$$

The arrangement of increment regions ($\mathrm{Re}\,p \geqslant 0$) is shown in Fig. 9a for those cases which have been realised in practice. Here, $k_3$ is chosen as the parameter defining the positive feedback level. Typical values of other parameters involved in the model are presented in Refs [83, 85]. More general conditions for autowave excitation are given in Ref. [43]. Fig. 9b shows the dependence of $\omega = (\mathrm{Im}\,p)^2$ on $K^2$ obtained for both systems when $\mathrm{Re}\,p = 0$, that is, at the boundary of the loss of stability.

The following conclusions can be drawn from the linear analysis:

1. The boundary between the stability region and the increment region as well as the dependence of $\omega^2$ on $K^2$ for the simplified system are not very different from those for more complex models. Therefore, having regard to the low accuracy of parameter measurements in living systems, the simplified equations (6.8) and (6.15) are quite adequate for most cases.

2. The increment region is bounded from above and the upper limit for the wave number can be obtained when elastic forces acting along the strand walls [see Eqn (6.9)] are taken into account.

3. The oscillation frequency is weakly dependent on the wave number when the system is in the vicinity of the excitation threshold. For a typical strand ($R = 0.25$ mm and $L = 0.3-60$ cm as an example), the oscillation period lies within the range 60–600 s. This range is the same as that shown by plasmodial strands in vivo.

### 6.5 Quasi-harmonic autowaves

If the linear theory permits the existence of only one wavelength with a growing amplitude, then unstable spatial mode loops appear at the ends of the isolated strand. Application of the Bogolyubov–Mitropolskii method in combination with the Bubnov–Galerkin procedure has allowed us to derive equations for slowly varying

amplitudes and phases, and to obtain the following approximate expression for the frequency of mode $n$:

$$\omega_n^2 = \frac{Eh(0.5k_1 + k_2 + k_4)}{\eta h + 16\mu/RK_n^2} + (0.5k_1 + k_2)k_4$$
$$\approx \frac{E}{\eta}(0.5k_1 + k_2 + k_4) \ . \qquad (6.26)$$

From this expression we notice that the dependence of $\omega_n$ on $K_n = \pi n/L$ $(n = 1, 2, 3, \ldots)$ is weak as $\eta h \gg 16\mu/RK_n^2$. In addition, according to this method a linear approximation can be used to definite the threshold of autowave excitation. Numerical estimates of the oscillation period and the amplitude as well as the phase shifts between the variables in question, $x(z, t)$, $c(z, t)$, $P_A(z, t)$, are in good agreement with experimental data.

### 6.6 Wave automodulation and quasi-stochastic regimes

As previously noted, behaviour of the plasmodium is not limited only to quasi-harmonic standing autowaves in the strands. Periodic contractile activity, appearing in the frontal sheet both of spreading plasmodia and of other amoeboid cells [20, 92], travels around the whole cell periphery and has a fundamental period of about 2 min. A 'second' rhythm of the activity with a period of 10–20 min frequently occurs. This manifests itself in modulation of the auto-oscillation (Fig. 10a). With the help of time lapse cinematography of migrating plasmodium we also observed that different parts of the frontal zone undergo successive extensive protrusions with a period of the second rhythm. These effects are described by computer simulations of the basic model for both the long strand and the plasmodial sheet.

The numerical simulation shown in Fig. 10b illustrates a standing wave in the strand when the linear analysis allows the existence of the first four unstable modes. The temporal oscillations of all variables differ considerably from harmonic oscillations. Their modulation is observed as a result of nonlinear interactions between the modes. The spatial pattern at fixed times shows that the amplitude of radial deviations, which is small in the middle part of the strand increases stepwise at its ends. The sharp loops seem to be precursors of the new frontal zones always occurring in excised real strands. The shape of the standing wave favours the 'two-compartment' mechanism of shuttle streaming. The flow velocity at each instant is practically constant along the middle part of the strand.

Autowaves in a circular strand for the case of instability of the first two spatial harmonics are shown in Fig. 10c. The quasi-stochastic character of the auto-oscillation depends on the form of the initial distributions. The boundary conditions obviously provide a wide diversity of possible regimes (from 'zero' tone to quasi-stochastic fluctuations). Fig. 11 shows the surface dynamics (the thickness changes) of a two-dimensional plasmodial disk-like sheet [93]. Its behaviour may also exhibit a wide variety of wave forms, because all the model solutions, rotated by any angle around the disk axis, are equally valid.

Another way of explaining a rotating lamellipodial protrusion wave around the cell periphery has been suggested by Alt [92, 94]. In contrast to ours, his model system does not need any additional control of contractility by calcium ions. The propagated autowave is induced by interaction of only two essential variables describing the

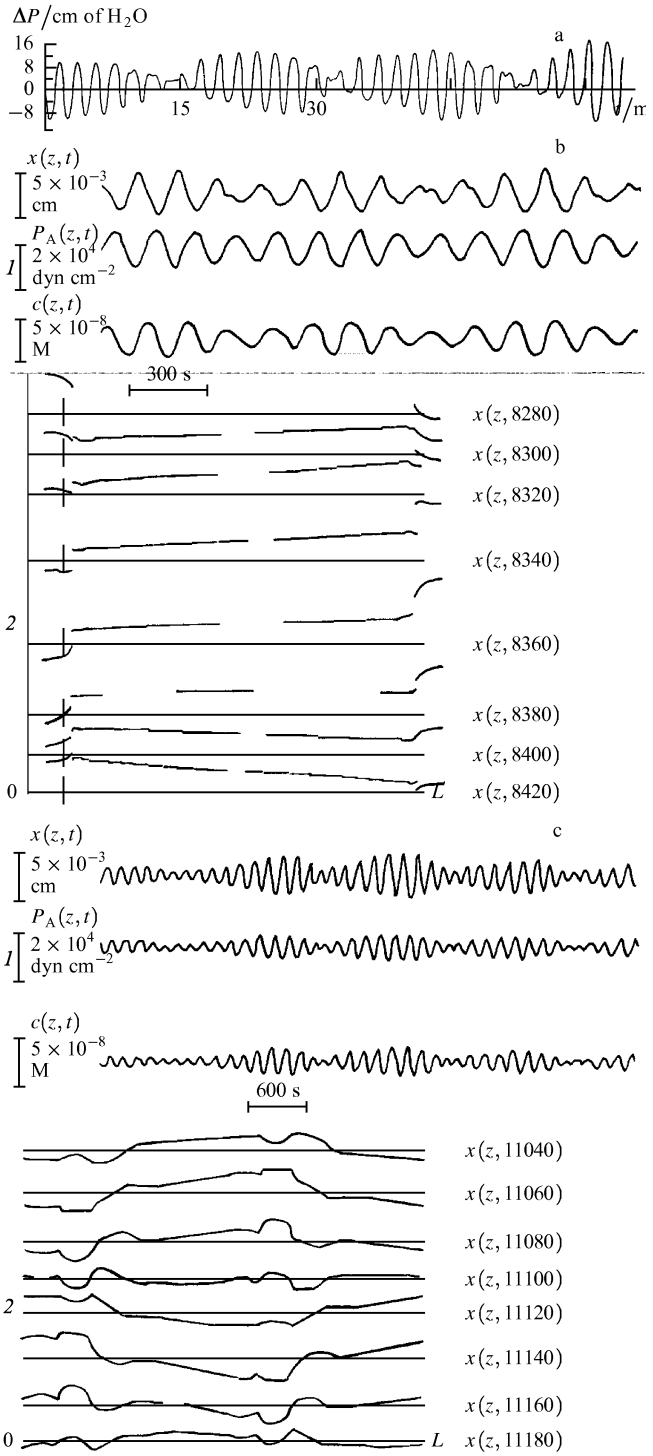


**Figure 10.** Real and simulated auto-oscillations in a strand fragment: (a) Typical pattern of modulated oscillations of the counter-pressure, $\Delta P$, applied to keep protoplasm in the central part of the strand at rest (from Ref. [112]). (b) Solutions of the model in the case of excitation of the first four modes. (c) Solutions for the case of excitation of the first two modes, but for the circular strand. (*1*) Oscillations of $x(z, t)$, $P_A(z, t)$, and $c(z, t)$ in the section $z = z' = 0.15L$, (*2*) distributions of $x(z, t)$ at fixed instants (obtained at 20 s intervals).

radial extension, $L(\varphi, t)$, of the cell periphery and the density, $n(\varphi, t)$, of the underlying cortical actomyosin layer. One important feature of the system on the unit circle is that stationary patterns might appear, but are stable only up to rotational shifts. To explain that

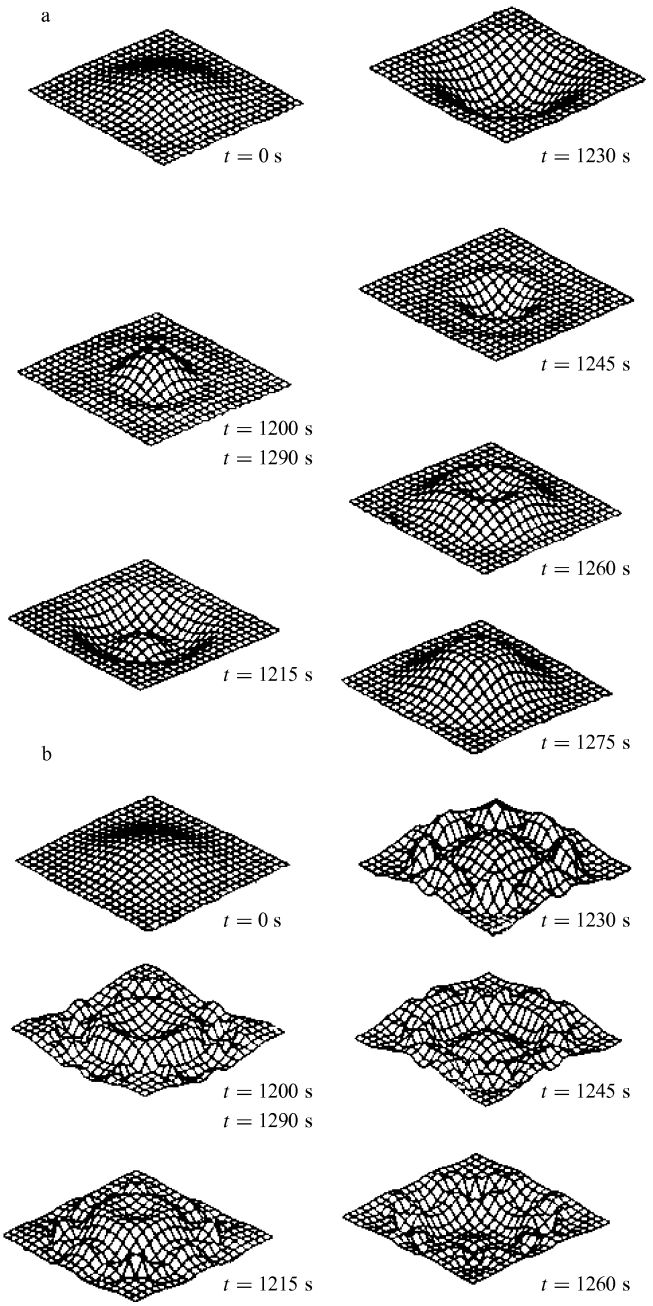


**Figure 11.** Surface dynamics of a spreading plasmodium at a small (a) and large (b) number of excited spatial harmonics for a system close to the boundary of the stability region.

protrusion patterns are shifted circumferentially the author introduces stochastic perturbations of the equation system. Noteworthy also are the recent works devoted to the appearance of mechanochemical waves on the surface of fertilised eggs. The propagation of surface contraction waves from the site of fertilisation is most pronounced in frog eggs [95]. Theoretical models have been constructed for the wave of calcium release that follows fertilisation and stimulates the contraction wave [96, 97].

The next step in the development of the models should include free moving boundary conditions, which could bring about an advance towards a consistent theory of amoeboid motility. Namely, the integration of the models of endoplasm streaming and pseudopodium extension with the models of autowave motility and regulation of cell migration by internal and external factors will allow the construction of a comprehensive theory of cell locomotion. At the same time such a theory should make it possible to explain nonautonomous regimes, when the cell as a whole is subjected to different external effects. Some examples of such a nonautonomous behaviour are considered below.

## 7. Physical methods for cell movement research

### 7.1 Cell tensiometry

A single cell is considered to be a rather difficult object for mechanical studies by the existing experimental techniques. The size of the majority of cells and, particularly, their local parts that are of interest to us is very small. The deformation fields are difficult to measure with sufficient accuracy by optical techniques because of light diffraction. In addition, the forces required to deform the cell are also small and difficult to control and measure. Over many years, for cell mechanics studies the methods of micropipette aspiration and compression between two plates have been applied. Glass microneedles and magnetic particles have been also used in the determination of mechanical properties of cellular components [98]. A high-resolution optical trap technique has recently been devised, which allows direct measurement of force and displacement that result from the interaction of a single myosin molecule with a single actin filament [99]. It has been shown that discrete stepwise movements averaging 11 nm are seen under conditions of low load, and single force transients averaging $(3-4)\times 10^{-12}$ pN are measured under isometric condition. These magnitudes are consistent with predictions of the theoretical models of muscle contraction [24]. Nevertheless, the mechanical study on a single cell remains a problem to be solved. In any event, the mechanical properties of cells are much less investigated than, for example, their electrical characteristics. In this respect, *Physarum* plasmodial strands, owing to their large sizes offer a unique opportunity for the investigation of mechanical and thermodynamic aspects of nonmuscle motility.

Plasmodial viscoelastic properties and their dependence on deformation at different phases of auto-oscillation were determined on the basis of the transient tension responses of the strand to rapid 1% length shortening [85, 100]. Such deformations do not cause a permanent change in the behaviour of the protoplasmic strands. The dynamics of responses could be divided into two phases. The initial force change occurred simultaneously with the applied length change and hence was an elastic response. After the step had been completed, there was a partial recovery towards the original tension level. This phase of the tension recovery was well fitted by a single exponential curve with a time constant of about 2 s (the regression coefficient was found to be $0.9988 \pm 0.0007$). Because the plasmodial strands are characterised by an inherent nonstationary tension, it is difficult to determine exactly the asymptotic value of force corresponding to the termination of recovery phase and needed for the calculation of viscoelastisity. Therefore, short (about 1 s) rectangular impulses of deformation were used. This time interval is much shorter than the period of auto-oscillations and the coefficients of stiffness and viscosity thus obtained may be considered as corresponding to a certain phase of auto-oscillations.

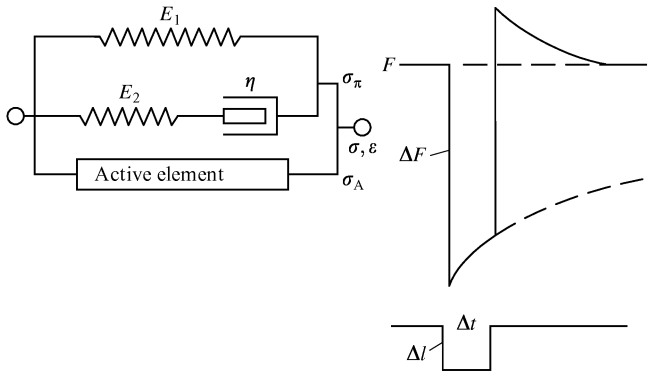


**Figure 12.** A rheological model of the strand wall and its response to a short deformation impulse.

The character of force responses allows us to depict the viscoelastic properties of the strand by the rheological model shown in Fig. 12. Solution of the simple differential equation describing the behaviour of this model on the application of a short rectangular impulse of deformation yields the following formulae for the calculation of the characteristics in question. The time constant $\tau$ is determined from the expression:

$$\tau = \frac{\Delta t}{\ln(1 + F'_{t2}/F'_{t1})}, \tag{7.1}$$

where $\Delta t$ is the duration of the deformation impulse, $F'_{t1}$ and $F'_{t2}$ are the time derivatives of the force at the beginning and the end of the deformation impulse, respectively. The stiffness coefficients are:

$$E_2 = \frac{\Delta F}{\Delta l}\left[1 + \exp\left(-\frac{\Delta t}{\tau}\right)\right], \qquad E_1 = \frac{\Delta F}{\Delta l} - E_2 , \tag{7.2}$$

where $\Delta F$ is the force step in response to the length change $\Delta l$. The viscosity coefficient is

$$\eta = E_2 \tau .$$

Fig. 13 shows the time courses of the longitudinal isometric force and the viscoelastic characteristics of the strand during one auto-oscillation period. They are seen to change synchronously; periodic elasticity oscillations observed earlier [63, 64, 102] are accounted for by the oscillations of the stiffness coefficient $E_1$ alone. The value of the stiffness coefficient $E_2$ is independent of the strand activity phase and seems to characterise purely the passive properties of the strand. It is noteworthy that the relationship between the instantaneous stiffness and the isometric force generated by the strand is linear. After the strand activation caused by 20% stepwise stretching, the stiffness coefficient $E_1$ increases within several seconds so that its new values fall again along the same straight line. The elastic modulus is apparently proportional to the number of cross-linkages in the network of actin filaments, and hence the variation of $E_1$ reflects the changes in the number of actomyosin complexes.

If we assume that the longitudinal force is determined only by the stress in the wall whose thickness amounts to 10% of the strand diameter, the stiffness and viscosity coefficients can be converted into the respective moduli of the ectoplasm. Thus the longitudinal Young's modulus calculated from the data in Fig. 13 is about $5 \times 10^5$ dyn cm$^{-2}$ in the phase of maximum relaxation of the strand and about

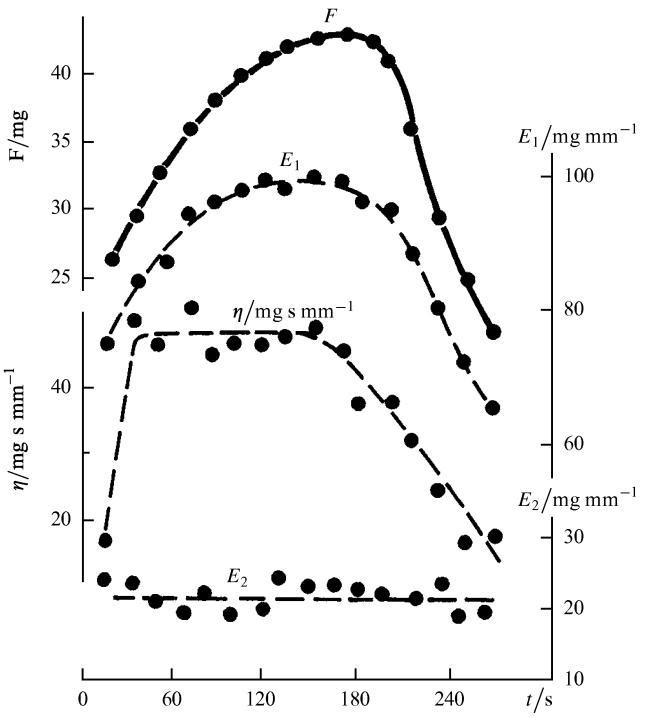


**Figure 13.** Spontaneous changes of force $F$ and mechanical parameters $E_1$, $\eta$, $E_2$ of the strand during one auto-oscillation period. The length and diameter of the strand are 5 and 0.7 mm, respectively.

$5 \times 10^6$ dyn cm$^{-2}$ in the phase of maximum contraction. The respective values of the viscosity coefficient in these phases of auto-oscillations are equal to about $2 \times 10^6$ and $4 \times 10^6$ P. To model a plasmodial migration, the rheological scheme should be supplemented with an appropriate viscosity element. The viscosity value, determined by the time of relaxation of the average level of strand tension, is of the order of $10^8$ P. On a time scale comparable to the auto-oscillation period this element may be neglected.

In the model (6.6) or (6.15), (6.20), (6.21) derived above we have assumed to a first approximation that the ectoplasm is isotropic and that the modulus values calculated for the phase of maximum relaxation correspond to the passive properties of the strand. The modulus augmentation is considered to be an attribute of the active element shown in Fig. 12.

### 7.2 Laser Doppler anemometry

The techniques of quasi-elastic laser light scattering spectroscopy have been applied widely for the study of dynamic characteristics of biological objects, in particular for the measurements of diffusion coefficients and velocities of directed movements (for example blood flow, bacterial motion, and intracellular protoplasm streaming) [103]. We shall focus here only on laser Doppler anemometry (LDA) which was used for the first time in 1974 by Mustacich and Ware [104] to study intracellular motility.

We know that the frequency of light scattered on a moving particle shifts, owing to the Doppler effect, by the value:

$$\Delta\omega_D = (\boldsymbol{V}, \Delta\boldsymbol{K}) , \tag{7.3}$$

where $\boldsymbol{V}$ is the particle velocity vector, $\Delta\boldsymbol{K}$ is the difference between the wave vectors of incident and scattered light.

Hence the Doppler frequency shift and the velocity of the particle are linearly related and the coefficient of proportionality depends only on the geometry of the optical scheme. The main difficulties with the use of LDA for measurements on cells are as follows: (i) the velocities of particles can be very small (a few micrometres per second); (ii) the measurement volume from which the scattered light is collected can contain many dissimilar particles moving with different velocities; (iii) owing to the heterogeneity of the cell material the laser beam can partly lose coherence; (iv) as the $\Delta\omega_D$ value can be of the order of 1 Hz, the output signal is mixed with low-frequency noises which modulate the intensity of the laser beam. In the general case the spectrum of the LDA output signal (without taking into account noise components) is given by the formula [105]:

$$S(\omega) = I(\theta) \int W(|V|)\, S_0\left(\frac{\omega - (V, \Delta K)}{|V|/r_k}\right) \mathrm{d}V \ . \qquad (7.4)$$

Here $I(\theta)$ is the index of laser beam scattering from the cell wall, $\theta$ is the angle of scattering, $W(|V|)$ is the function of the velocity distribution of the scatterers in the channel, $r_k$ is the radius of correlation of probing wave within the measurement volume, $S_0$ is the Fourier image of the correlation function of the probing wave field within the channel. Thus the resulting spectrum represents a superposition of the broadened spectra obtained from individual particles. The degree of spectrum broadening is determined by the time-of-flight, $T = r_k/V$, through the region within which the field of the probing wave is spatially coherent. It should be also emphasised that intracellular flows are nonstationary. For example, for *Physarum* the flow velocity must be measured several times during a single period lasting only 1–3 min.

Therefore, the simplest one-beam scheme gives an output signal whose power may be thought of as being proportional only to an effective value of the velocity modulus (Fig. 14). At the same time, such a form of $P(t)$ allows the value of the period to be determined with good accuracy and therefore also the values of the time intervals $\tau_1$ and $\tau_2$ ($\tau_1 + \tau_2 = T$), when endoplasm streams in one or the other direction. This has allowed us to determine quickly and reliably the dependences of the period on temperature, light, etc. The results presented in Section 8 were obtained by this very simple scheme. It should be mentioned that a multichannel LDA has been designed on the basis of several one-beam schemes operated in parallel [106].

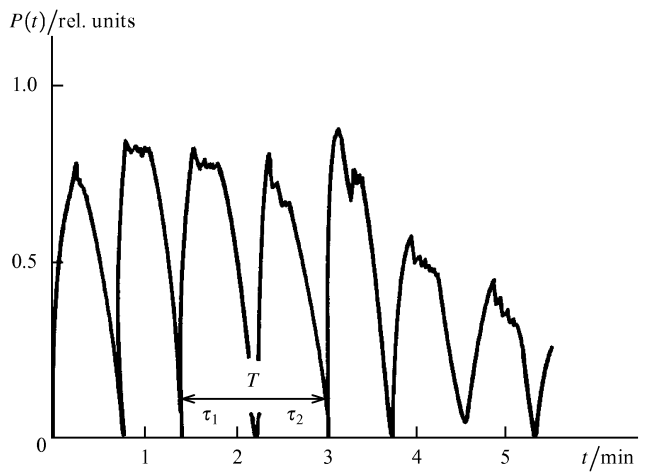


**Figure 14.** Oscillations of LDA signal power at the integrator output.

Studying intracellular movements imposes the following demands on LDA:

1. Measurement of flow velocities from a few to several hundred micrometres per second.
2. Space resolution down to 5 μm.
3. Real-time measurement of velocities of nonstationary flow.
4. The intensity of probing radiation less than 1 mW $m^{-2}$.
5. Wavelength $\lambda \approx 600$ nm (its influence on cells is much less than that of the blue–green part of the spectrum).
6. Computer control and data processing. Compatibility with instruments measuring voltage, membrane potential, etc.

### 7.3 Laser Doppler microscope

Laser Doppler microscopes, LDM, designed in several countries [107, 108] satisfy the listed requirements in many respects. We shall describe here the sign-sensitive scanning LDM devised by A V Priezzhev, V N Glonty and, S G Proskurin at the Physical Faculty of Moscow University on the basis of the luminescence microscope YUMAM-R1 [103, 109–111].

The beam generated by the He–Ne laser (LG-79-1, output of 10–15 mW) is split into two similar beams and directed into acousto-optical modulators (AOM) operating in the Bragg regime. Beams corresponding to +1 diffraction order are used at their output. The excitation frequencies of AOM generators are $f_1 = 50$ MHz and $f_2 = f_1 + \Delta f$, where $\Delta f = 1$ kHz. With the aid of a focusing system the beams are made to intersect inside a transparent living object and form the measurement volume. Within the measurement volume there appears a travelling interference pattern. A computer-controlled motor attached to a thermostatted stage permits scanning the object in the horizontal direction. When a scatterer crosses the interference bands, the Doppler shift, $\Delta\omega_D$, depends on the direction of motion, which permits sign-sensitive recording of the scatterer velocity. Such records are not affected by low-frequency laser noises. Using different objectives one can obtain characteristic sizes of the measurement volume in the range of 5–10 μm. In addition, the distribution of scatterer concentrations across the stream can be obtained from measurements of the Doppler signal intensity.

With the aid of the LDM it has been possible to investigate nonstationary protoplasm streams with velocities as low as a few micrometres per second (Fig. 15a). The data can be subjected to additional computer processing and presented in a convenient form (Fig. 15b). In this way non-Newtonian velocity profiles of shuttle protoplasmic flows in the plasmodial strands have been determined (Fig. 16).

In principle, departures of the profile from parabolic shape can be taken into account in the construction of mathematical models. Analysis of the intensities of Doppler spectrum components has shown that the scatterer distribution density is nearly uniform across the channel. Some of these results could be obtained with the aid of other, much more cumbersome techniques. For example, a photoframe taken with light-microscope magnification at long

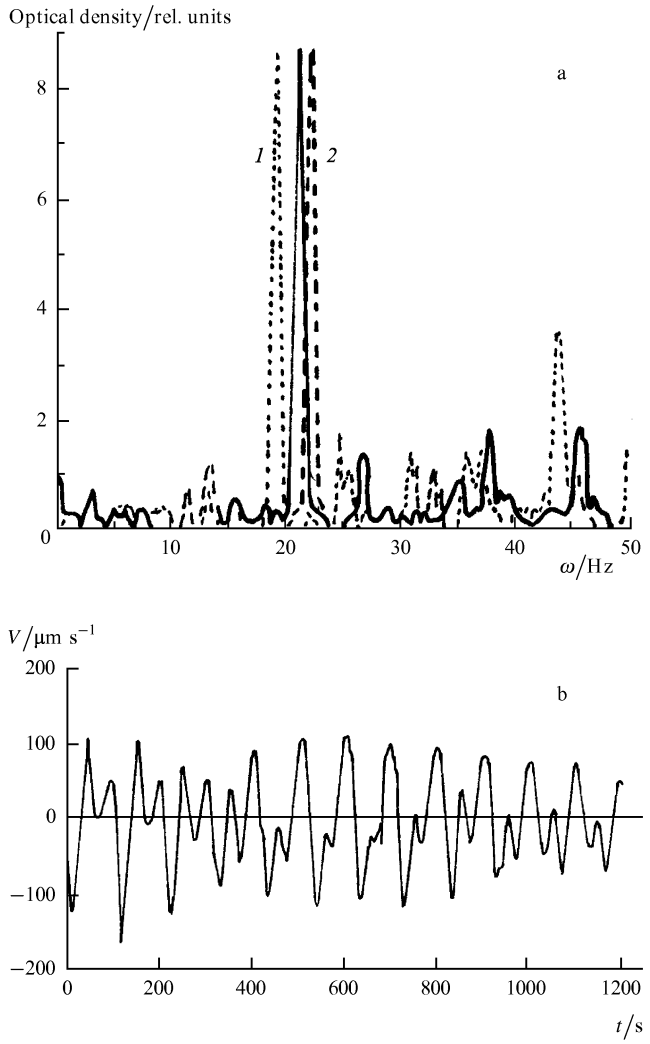


**Figure 15.** (a) Doppler spectra representing the velocity resolution of LDM. A scattering film has been used as the object. Peaks correspond to velocities of −2, 0, and +1 μm $s^{-1}$. (b) Temporal dependence of the endoplasmic flow velocity at the axis of a plasmodial strand.

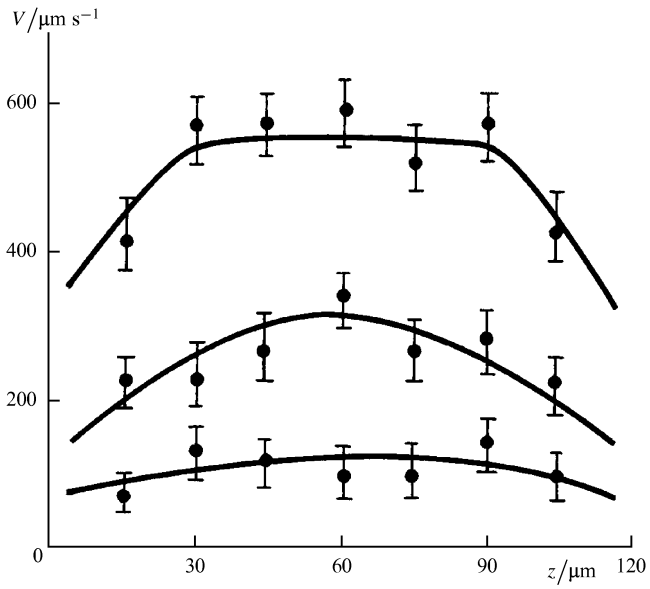


**Figure 16.** Profiles of endoplasm flow velocity obtained by scanning a plasmodial strand at different times.

exposure could be used [112] to measure velocities by processing trace lengths of separate moving particles. However, this does not compare with the simplicity and convenience of the LDM use. The determination of velocity with the help of LDM can be made simultaneously with diameter measurements of several strand sections and with monitoring of the force generated by the strand [52, 56].

Below we shall describe the motile responses of *Physarum polycephalum* plasmodium to various external influences revealed with the use of this technique. The study of nonstationary effects allows us to understand how this remarkable self-organising living machine operates and to refine further the corresponding mathematical models. We shall begin the description with the influence of temperature on the plasmodial motive behaviour.

## 8. Nonstationary external influences as a way of studying oscillatory motility

### 8.1 Synchronisation of shuttle protoplasmic movement by periodical changes of the temperature gradient

It is well known that protein molecules and living cells maintain their capability for normal functioning over a temperature range from 10 to 40 °C. The *Physarum* plasmodium reacts to temperature variations in the environment by changes in the oscillatory contractile activity and the velocity of protoplasm flow. In the presence of a spatial temperature gradient it changes the direction of its movement [58, 112]. As the temperature is increased the period of shuttle streaming decreases. Wohlfarth-Bottermann investigated the dependence of the auto-oscillation period on temperature with the aid of tensiometry [113] and Kolin'ko et al. [114] have taken a further look at this dependence using LDA (Fig. 17). They

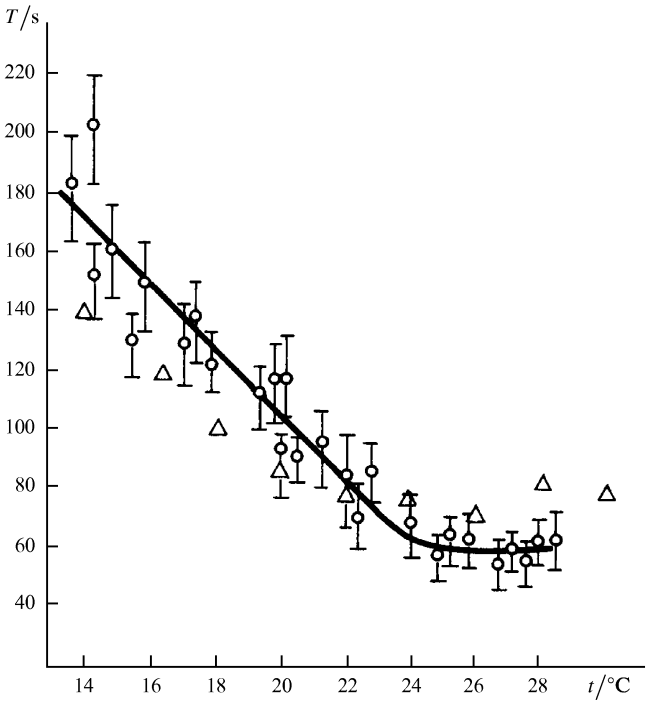


**Figure 17.** Temperature dependence of the contractile oscillation period. Circles mark the averaged period values with standard deviations shown by vertical bars. Triangles show data obtained in Ref. [113].

have also determined the kinetics of changes of the shuttle flow period occurring in response to temperature shifts applied externally.

Study of the time course of the auto-oscillation period after stepwise changes in temperature has led to the following results [114]: (i) the period of plasmodial oscillator reacts to temperature shifts practically at once; (ii) as the temperature drops from 21 to 17 °C the period passes through a large maximum and reaches a stationary level in about 1 h, whereas when the temperature is increased it reaches a stationary level in as little as 3 min. These data were interpreted on the assumption that sharp cooling enhances gelation which could be the reason for the initial increase in the period duration. The subsequent prolonged decrease in the period duration down to values corresponding to the new stationary regime can be ascribed to the activation of proteins capable of inhibiting actin polymerisation or/and gel formation processes.

As is evident from the foregoing, the plasmodial strand is an autowave system in which periodical changes of the gradient of intracellular pressure cause shuttle protoplasmic streaming. Because the spatially nonuniform temperature conditions affect gradients of the intracellular pressure, rhythmical changes in the temperature gradient would act as an application of a periodic gradient of intracellular pressure. Such an influence has been found to result in the entrainment of autowave flows [114]. This process is demonstrated in Fig. 18. A plasmodial strand was placed in a two-compartment thermostat so that each end was located in one of the compartments. The mean temperature in the compartments was maintained at around 19 °C. The maximal value of the temperature gradient in an oscillation cycle was equal to 0.5 °C $cm^{-1}$. The period of the temperature gradient oscillation changed discretely with a 10 s step in 40 min. It is seen that the entrainment is attained when the period $T = 100$ s and $T = 110$ s (as well as at any periods inside this interval), but at $T = 120$ s the entrainment is no longer observed. So, the plasmodium represents a peculiar autowave system capable of entrainment by external periodic influences. It should be noted that the plasmodial oscillator is also capable of pulling the frequency of periodically applied external pressure gradient

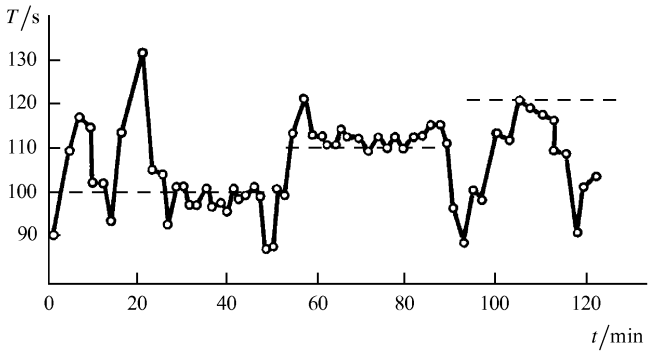


**Figure 18.** Entrainment of the flow velocity oscillations by a periodically changing temperature gradient. Experimental points connected by lines correspond to instantaneous values of the velocity oscillation period. Dashed lines indicate the duration and the period of the temperature oscillation. At $T = 100$ s and 110 s the entrainment is seen to occur but at $T = 120$ s a beat-like frequency modulation arises.

[74]. The experiments carried out with LDA have also shown that two interconnected protoplasmic strands having different initial frequencies synchronise through the protoplasm flow [34, 52]. Unfortunately, mathematical models of the synchronisation are not yet available.

### 8.2 The effect of light on plasmodium autowave regimes

Thousands of studies are devoted to the effect of light on photosynthesising plant cells and retina photoreceptors. Photoreactions of cells that lack a sensory mechanism of so high a degree of perfection have been much less investigated. Large intensities and high doses of illuminations induce damage and often lead to cell death, whereas low doses control a variety of behavioural reactions. Among other responses, amoeboid cells are capable of exhibiting phototaxis. It is expressed in their migration along the gradient of light intensity. Cells are most sensitive to the blue part of the spectrum. However, the mechanism of blue light photoreception remains obscure [115]. For the light-induced motile response of *Physarum* plasmodium such is indeed the case [116–118], though it is known that the period of shuttle streaming changes considerably on modification of the light regime [119]. It should be mentioned that this response is very specific with respect to the spectrum of the applied light [120, 121], which provides an opportunity for studying the photoreception mechanism.

Fig. 19 shows changes in the period of flow velocity oscillations in response to laser illumination of various wave-lengths. The data were obtained with the aid of LDA [121]. It is seen from these curves that about 1 h after the start of light exposure an adaptation occurs manifesting itself in the return of the period value to that observed in darkness. The kinetics of the response exhibit a series of well-defined local maxima, which are only weakly dependent on the wavelength of illumination. It follows from the insert in Fig. 19a that the integral effect has a maximum at $\lambda = 460$ nm. Similar responses are formed in many other cells [122]. The curves of evolution of the auto-oscillation period at various durations of the light exposure are shown in Fig. 19b. The important feature of these dependences is that the period duration decreases below the control value when the illumination is cut off. In the next paragraph we shall formulate a mathematical model that offers some explanation of the observed effects and may give an impetus to new experiments on the amoeboid cell photoreactions.

### 8.3 Mathematical model of a nonautonomous system

Equations (6.8) (6.20) (6.22) describing the endoplasmic autowave flow in plasmodial strands will form the basis for the nonautonomous model. Effective parameters of the model $k_i$ $(i = 1-4)$ can be dependent on the kinetics of many biochemical processes. They control the period of shuttle protoplasmic streaming when all the other parameters are constant [see Eqn (6.26)]. The first step of modeling made by Pavlov et al. [123] was the elucidation of the quantitative dependences the auto-oscillation period, obtained by a computer simulation of the basic model, on the values of these parameters. The parameter values were chosen in such a way that the condition of self-excitation for the first spatial mode would remain in force. The parameter $k_1$ responsible for the startup of the actomyosin complex formation has the strongest influence on the auto-oscillation period. A preliminary computer experiment has shown that a stepwise

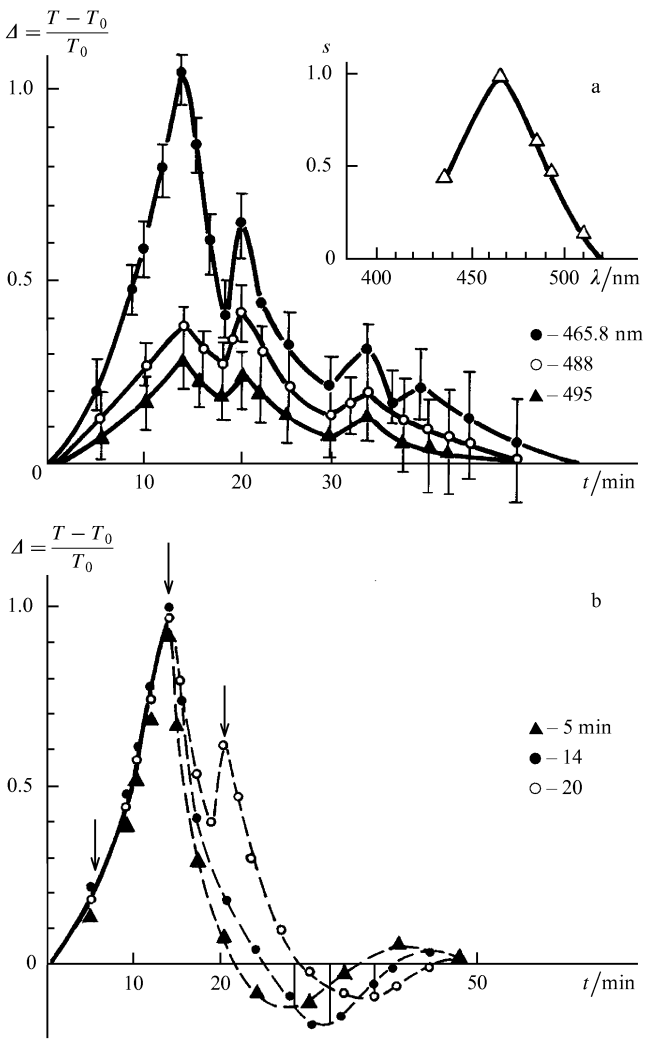


**Figure 19.** Changes in the auto-oscillation period of the plasmodium: (a) on continuous illumination by monochromatic light [the insert shows the dependence of the integral effect — the area under the curve $\Delta(t)$ — on the emission wavelength]; (b) at different durations of illumination and $\lambda = 465.8$ nm. The arrows indicate the instants of switching off the light; $t = 0$ corresponds to the beginning of illumination. $T_0$ is the averaged period before the illumination. $T$ is the current period. The irradiance at the sample was 4 W m$^{-2}$.

change in $k_1$ results in fast (over one period) establishment of a new oscillation frequency. Therefore, it was postulated that a time-dependent function $k_1(t)$ could be found which would define the required change in the period duration as the time-dependent coefficient of the basic system. This was attempted with the help of squared spline approximation of the photoreaction curve at $\lambda = 465.8$ nm shown in Fig. 19a and of the function $T_0(k_1)$. The results are shown in Fig. 20.

Then, as a first approximation, we tried to adopt such a scheme of biochemical processes (beginning with an excitation of plasmodial photoreceptory pigment and ending with the change in activator concentration proportional to $k_1$) which could ensure the required dependence. Certainly, other variants cannot be excluded, but in any case modeling allows one to check whether the suggested scheme is realistic, thus leading to more effective experimental search. It is obvious that the function $k_1$ can in turn be approximated by the following expansion:

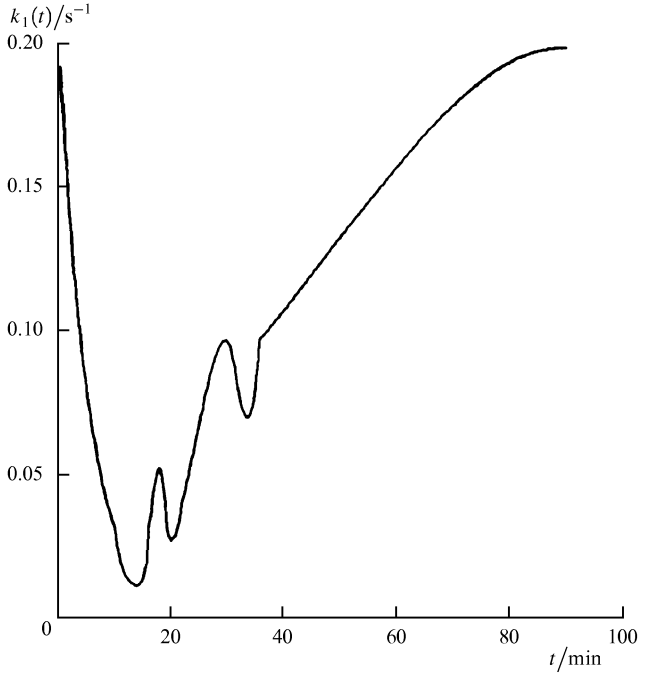


**Figure 20.** Evolution of the parameter $k_1(t)$ in time, found on modeling the plasmodium photoreaction.

$$k_1(t) - \bar{k}_1 = A \exp\left(-\frac{t}{\tau}\right) + B \exp\left(-\frac{t}{\tau}\right) \sin(\Omega t + f) + C \exp(-\delta t) \,. \tag{8.1}$$

Here $\bar{k}_1$ is the stationary value in the absence of illumination, $\delta^{-1}$ is the time of adaptation (a few minutes), which was shown to coincide with the time it takes for the intracellular medium to acidify [121]. An adaptation under the effect of light is also observed in the plasmodium and many other cells sensitised by various dyes [122].

The most plausible hypothesis is that, excited by light and interacting with membrane proteins, an endogenous plasmodial photoreceptor (putatively of flavin nature [124]) promotes the production of special metabolites — second messengers. Cyclic nucleotides are most likely to be involved in this process as the second messengers [125, 126]. In this model we assumed that the protoplasm acidification or cyclic nucleotides decrease $k_1$ and possibly have an influence on other $k_i$. As the function $k_1(t)$ has along with the exponentially damping terms a periodically varying one, it is necessary to assume the existence of an activator — the second variable — connected with the inhibitor so that auto-oscillations would arise. As all 'dramatis personae' are not yet exactly known, the following system of kinetic equations may be suggested:

$$\begin{aligned} \frac{\partial y_1}{\partial t} &= a_{10} D_0 \exp\left(-\frac{t}{\tau}\right) - a_{11} y_1 - a_{12} y_2 \,, \\ \frac{\partial y_2}{\partial t} &= a_{20} D_0 \exp\left(-\frac{t}{\tau}\right) + a_{21} y_1 \,, \\ \frac{\partial k_1}{\partial t} &= \frac{\gamma_1(\bar{y}_1 + y_1)}{\gamma_2 + \bar{y}_2 + y_2} - \delta k_1 \,, \quad t > 0 \,, \\ y_1(0) &= \bar{y}_1 \,, \quad y_2(0) = \bar{y}_2 \,, \quad k_1(0) = \bar{k}_1 \,. \end{aligned} \tag{8.2}$$

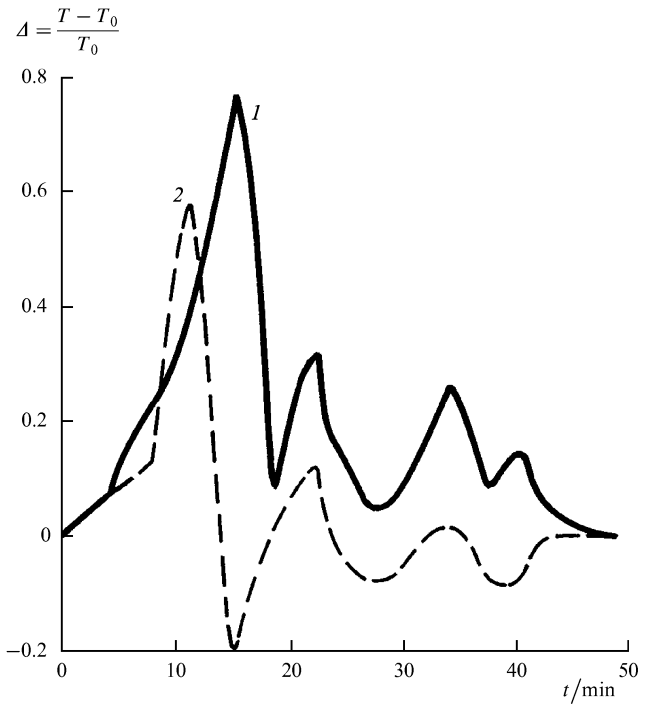


**Figure 21.** The predictions of the linearised model for the changes in the auto-oscillation period in response to a continuous light illumination of the plasmodium (curve *1*) and in response to a 5 min illumination pulse (curve *2*).

Here $\bar{y}_1$ and $\bar{y}_2$ are the concentrations of the activator and the inhibitor in darkness, respectively. $y_1$ and $y_2$ are their deviations from $\bar{y}_1$ and $\bar{y}_2$ under illumination. $D_0$ denotes the photoreceptor activity and $\tau$ is its relaxation time. The coefficients $\alpha_{10}$ and $\alpha_{20}$ depend on the radiation wavelength. The first two equations in (8.2) can be considered as a linear analog of Volterra's population model. The third equation is an analog of Michaelis–Menton kinetics for an enzyme–substrate–inhibitor system describing the transformation of 'substrate' $y_1$ into 'product' $k_1$ with the participation of inhibitor $y_2$.

Without light there is a stationary regime. All the derivatives are equal to zero and the value of $k_1$ determines the auto-oscillation period in darkness. Curve *1* in Fig. 21 describes a light-induced change of the period duration simulated by our basic model (6.8) (6.20) (6.22) in the case when the parameter $k_1(t)$ is defined by the linearised system (8.2). This solution is quite satisfactorily fitted to the experimental data shown in Fig. 19a. In addition the linearised model qualitatively describes changes in the oscillation period under brief light illumination (compare curve *2* in Fig. 21 with the curves in Fig. 19b). It should be emphasised that, in spite of satisfactory results obtained by the linear approach, the choice of an appropriate nonlinear model remains ambiguous and new experiments with living plasmodia are required. For example, light illumination could be applied simultaneously with substances which change this or another stage of plasmodial photoreaction. Although solutions of the linearised model (8.2) are physically plausible only for the case of small deviations of $y_1$ and $y_2$ from the stationary values, nevertheless the possibility to explain satisfactorily new nontrivial oscillatory regimes in the cell motile behaviour counts in favour of the elaborated model.

## 9. Conclusion

It can be seen that at present the theory of amoeboid motility is constructed only in fragments. A major problem to be tackled in the nearest future is the integration of separate models into a single mathematical description covering both the self-organisation of intracellular movements and the cell migration. It is impossible here to dispense with the principles of directional movement control developed in the theories of cell-to-cell communications and self-organisation of collective behaviour in cell populations. The state of researches in this field has been described in a recent review [127]. It should be remembered that the majority of animal tissue cells exhibit the amoeboid type of motility, so elucidating physical principles of their locomotion is of importance both for the theory and for medical applications. It is essential to make progress in the understanding the self-organisation of processes in acto-myosin networks. It is necessary to realise the important role of strains and stresses in the control of cell motility and elucidate the interplay between this kind of control and other cell regulatory pathways. From the synergetic viewpoint the exciting problem is how the optimal form of migrating amoeboid cells is attained and which intracellular parameters define this process. For modeling this kind of patterning it is necessary to find an optimality criterion which could be formulated in the context of the theory of open nonequilibrium systems.

For experimental studies of cell motility new opportunities have appeared with the advent of confocal microscopy, fluorescent probes, optoelectronic amplifiers, holography, and other optical techniques. Worthy of mention is also a new promising method of laser phasic microscopy [128]. The use of these methods could be combined with the laser Doppler technique which enables the dynamic characteristics of protoplasmic flows to be measured. The use of new empirically determined parameters will provide much scope for improvement of the existing mathematical models and further development of the theory.

**Acknowledgements.** We are grateful to the Russian Foundation for Fundamental Research for financial support (Grant No. 94-04-12233) and to Dr Micah Dembo (Theoretical Division, Los Alamos National Laboratory, USA) for reading the manuscript and helpful remarks.

## References

1. Nicolis G, Prigogine I *Self-Organization in Non-equilibrium Systems* (New York: Wiley, 1977)
2. Haken H *Advanced Synergetics. Instability Hierarchy in Self-Organizing Systems and Devices* (Berlin: Springer, 1983)
3. Ebeling W *Strukturbildung bei Irreversiblen Prozessen* (Leipzig: Teubner, 1976)
4. Vasil'ev V A, Romanovskii Yu M, Yakhno V G *Avtovolnovye Protsessy* (Autowave Processes) (Moscow: Nauka, 1987)
5. Klimontovich Yu L *Statistical Theory of Open Systems: A Unified Approach to Kinetic Systems* (Dordrecht: Kluwer, 1995)
6. Kadomtsev B B *Usp. Fiz. Nauk* **165** 449 (1994) [*Phys. Usp.* **37** 425 (1994)]
7. Zhabotinskii A M *Kontsentratsionnye Avtokolebaniya* (Concentration Auto-oscillations) (Moscow: Nauka, 1974)
8. Ivanitskii G R, Krinskii V I, Sel'kov E E *Matematicheskaya Biofizika Kletki* (Mathematical Biophysics of the Cell) (Moscow: Nauka, 1978)

9. Belintsev B N *Fizicheskie Osnovy Biologicheskogo Formoobrazovaniya* (Physical Bases of Biological Pattern Formation) (Moscow: Nauka, 1991)
10. Akhromeeva T C, Kurdyumov S P, Malinetskii G G, Samarskii A A *Nestatsionarnye Struktury i Diffuzionnyi Khaos* (Nonstationary Structures and Diffusive Chaos) (Moscow: Nauka, 1992)
11. Kerner B S, Osipov V V *Avtosolitony* (Autosolitons) (Moscow: Nauka, 1991)
12. Karlov N V, Kirichenko N A, Luk'yanchuk B S *Lazernaya Termokhimiya* (Laser Thermochemistry) (Moscow: Nauka, 1992)
13. Lackie J M *Cell Movement and Cell Behaviour* (London: Allen & Unwin, 1986)
14. Blyumenfel'd L A *Problemy Biologicheskoi Fiziki* (Problems of Biological Physics) (Moscow: Nauka, 1977)
15. Chernavskii D S, Khurgin Yu I, Shnol' S E *Mol. Biol. (Moscow)* **1** 419 (1967); **20** 13 (1987)
16. Mast S O *J. Morphol. Physiol.* **41** 347 (1926)
17. Allen R D *Cell* **2** 135 (1961)
18. Grebecki A *Intern. Rev. Cytol.* **148** 37 (1994)
19. Trinkaus J P *Cells into Organs* (Englewood Cliffs, NJ: Prentice-Hall, 1984)
20. Smolyaninov V V, Bliokh Zh L, in *Nemyshechnye Formy Podvizhnosti* (Nonmusclar Forms of Motility) Ed. G M Frank (Pushchino: NTsBI Akad. Nauk SSSR, 1976) p. 5
21. Abercrombie M, Heaysman J E, Pegrum S M *Exp. Cell Res.* **67** 359 (1971)
22. Vasiliev Ju M, Gelfand I M, in *Locomotion of Tissue Cells* (Ciba Found. Symp., 1973) Vol. 14, p. 311
23. Weiss P *Exp. Cell Res. Suppl.* **8** 260 (1961)
24. Deshcherevskii V I *Matematicheskie Modeli Myshechnogo Sokrashcheniya* (Mathematical Models of Muscle Contraction) (Moscow: Nauka, 1977)
25. Bagshaw B *Muscle Contraction* (London: Chapman Hall, 1993)
26. Oster G F, Odell G M *Physica D* **12** 333 (1984)
27. Oster G F *J. Embryol. Exp. Morph. Suppl.* **83** 329 (1984)
28. Oster G F, Perelson A S *J. Math. Biol.* **21** 383 (1985)
29. Zhu C, Skalak R *Biophys. J.* **54** 1115 (1988)
30. Dimilla P A, Barbee K, Lauffenburger D A *Biophys. J.* **60** 15 (1991)
31. Dembo M, Harlow F, Alt W, in *Cell Surface Dynamics. Concepts and Models* (Eds S Parleston, Ch DeLisi, F M Wiegel) (New York: Marcel Dekker, 1984) p. 495
32. Alt W, in *Biomechanics of Active Movement and Deformation of Cells* (Ed. N Akkas) (Berlin: Springer, 1990) p. 403
33. Evans E *Biophys. J.* **64** 1306 (1993)
34. Beylina S I, Matveeva N B, Priezzhev A V, Romanovsky Yu M, Sukhorukov A P, Teplov V A, in *Self-Organization. Autowaves and Structures far from Equilibrium* (Ed. V I Krinsky) (Berlin: Springer, 1984) p. 218
35. Potapova O O, Beilina S I, Zaikin A N, in *Teoreticheskie i Matematicheskie Problemy Morfogeneza* (Theoretical and Mathematical Problems of Morphogenesis) (Ed. A I Zotin) (Moscow: Nauka, 1987) p. 86
36. Ivanitskii G R, Medvinskii A B, Tsyganov M A *Usp. Fiz. Nauk* **161** 13 (1991) [*Sov. Phys. Usp.* **34** (4) 289 (1991)]
37. Oster G F, Perelson A S *J. Cell Sci. Suppl.* **8** 35 (1987)
38. Oster G F, Perelson A S, Tilney L G *J. Math. Biol.* **15** 259 (1982)
39. Perelson A S, Coutsias E A *J. Math. Biol.* **23** 361 (1986)
40. Tilney L G, Inone S *J. Cell Biol.* **93** 820 (1982)
41. Dembo M *Biophys. J.* **55** 1053 (1989); Dembo M, in *Biomechanics of Active Movement and Division of Cells* NATO ASI Ser. H: Cell Biology, 84 (Ed. N Akkas) (Berlin: Springer, 1994) p. 231
42. Romanovskii Yu M, Chernyaeva E B, in *Termodinamika Neobratimykh Protsessov* (Thermodynamics of Irreversible Processes) (Ed. A I Lopushanskaya) (Moscow: Nauka, 1987) p. 152
43. Romanovskii Yu M *Mat. Model. (Moscow)* **8** 3 (1993)
44. Wohlfarth-Bottermann K E *J. Exp. Biol.* **81** 15 (1979)
45. Turing A M *Philos. Trans. R. Soc. Lond. B* **237** 37 (1952)
46. Kirber M T, Walsh Jr J V, Singer J J *PfluSgers Arch.* **412** 339 (1988)
47. Kolega J *J. Cell Biol.* **102** 1400 (1986)
48. Sandy J R, Meghji S, Farndale R W, Meikle M C *Biochem. Biophys. Acta* **1010** 265 (1989)
49. Ben–Ze'ev A, in *Cell and Muscle Motility* (Ed. J W Shay) (New York: Plenum, 1985) Vol. 6, p. 23
50. Barany K, Rokolya A, Barany M *Biochem. Biophys. Res. Commun.* **260** 7126 (1988)
51. Belousov L V *Biologicheskii Morfogenez* (Biological Morphogenesis) (Moscow: Moscow University Press, 1987)
52. Teplov V A, Beilina S I, Evdokimov M V, Priezzhev A V, Romanovskii Yu M, in *Avtovolnovye Protsessy v Sistemakh s Diffuziei* (Autowave Processes in Systems with Diffusion) (Ed. M T Grekhova) (Gorky: IPF Akad. Nauk SSSR, 1981) p. 190
53. Grebecki A, Cieslawska M *Cytobiologie* **17** 335 (1978)
54. Stewart P A, Stewart B I *Exp. Cell Res.* **17** 44 (1959)
55. Stewart P A, Stewart B I *Nature (London)* **192** 1206 (1961)
56. Ermakov V G, Priezzhev A V *Biofizika* **29** 100 (1984)
57. Baranowski Z, in Ref. [20] p. 47
58. Hejnowicz Z, Wohlfarth-Bottermann K E *Planta* **150** 144 (1980)
59. Teplov V A, Matveeva N B, Zinchenko V P, in *Biofizika Zhivoi Kletki* (Biophysics of the Living Cell) (Ed. G M Frank) (Pushchino: NTsBI Akad. Nauk SSSR, 1973) Vol. 4, p. 110
60. Kuroda R, Hatano S, Hiramoto Y, Kuroda H *Protoplasma Suppl.* **1** 72 (1988)
61. Nakamura S, Kamiya N *Cell Struct. Funct.* **10** 133 (1985)
62. Ueda T, Matsumoto K, Akitaya T, Kobatake Y *Exp. Cell Res.* **162** 486 (1986)
63. Kamiya N, Yoshimoto Y, in *Aspects of Cellular and Molecular Physiology* (Ed. K Hamaguchi) (Tokyo: University of Tokyo Press, 1972) p. 167
64. Teplov V A, Budnitskii A A, in Ref. [59] p. 165
65. Lairand D B, Matveeva N B, Teplov V A, *The Analysis of Protoplasm Movement in the Myxomicete Plasmodium. Intracellular Hydrostatic Pressure and Its Role in the Protoplasm Movement* paper No. 2001-70 deposited in VINITI, Moscow, 1970 [in Russian]
66. Layrand D B, Matveeva N B, Teplov V A, Beylina S I *Acta Protozool.* **11** 339 (1972)
67. Matveeva N B, Beilina S I, Teplov V A, Lairand D B, Lednev V V *Regulation of Taxis in Myxomicete Plasmodium* paper No. 2112-81 deposited in VINITI, Moscow, 1981 [in Russian]
68. Matveeva N B, Beilina S I, Teplov V A, Lairand D B, in *Nemyshechnye Dvigatel'nye Systemy* (Nonmuscle Motile Systems) (Moscow: Nauka, 1981) p. 155
69. Teplov V A, Beylina S I, Matveeva N B, Layrand D B, in *Progress in Protozoology* (Warsaw, 1981) p. 363
70. Yoshimoto Y, Kamiya N *Protoplasma* **95** 89 (1978)
71. Achenbach U, Wohlfarth-Bottermann K E *Planta* **151** 574 (1981)
72. Achenbach U, Wohlfarth-Bottermann K E *Planta* **151** 584 (1981)
73. Yoshimoto Y, Kamiya N *Protoplasma* **95** 89 (1978)
74. Kishimoto U *J. Gen. Physiol.* **41 1205** (1958)
75. Baranowski Z, Teplov V A *Cell Biol. Int. Rep.* **16** 1091 (1992)
76. Arkhangel'skaya T A, Barch G, Kolin'ko V G, Romanovskii Yu M, in *Dinamika Kletochnykh Populatsii* (Dynamics of Cellular Populations) (Gorky: Gorky State University Press, 1984) p. 98
77. Odell G M *J. Embryol. Exp. Morphol. Suppl.* **83** 261 (1984)
78. Oster G F, Odell G M *Cell Motility* **4** 469 (1984)
79. Romanovskii Yu M, Teplov V A, in *Matematicheskie Mekhanizmy Tubulentnosti* (Mathematical Mechanisms of Turbulence) (Kiev: IM Akad. Nauk Ukr. SSR, 1986) p. 103
80. Romanovskii Yu M, Khors N P *Biofizika* **27** 707 (1982)
81. Vasilyev V A, Romanovsky Yu M, Chernavsky D S, Yakhno V G *Autowave Processes in Kinetic Systems. Spatial and Temporal Self-Organization in Physics, Chemistry, Biology and Medicine* (Dordrecht: Reidel, 1987)

82. Romanovsky Yu M, Teplov V A, in *Thermodynamics and Pattern Formation in Biology* (Eds I Lamprecht, A I Zotin) (Berlin: De Gruyter, 1988) p. 395
83. Teplov V A, Romanovsky Yu M, Latushkin O A *Biosystems* **24** 269 (1991)
84. Latushkin O A, Netrebko N B, Romanovsky Yu M, Teplov V A, in *Kollektivnaya Dinamika Vozbuzhdenii i Strukturoobrazovaniya v Biologicheskikh Tkanyakh* (Collective Dynamics of Excitations and Pattern Formation in Biological Tissues) (Ed. V G Yakhno) (Gorky: IPF Akad. Nauk SSSR, 1988) p. 109
85. Teplov V A, Romanovsky Yu M *Mekhanokhimicheskie Raspredelennye Avtokolebaniya v Kletochnoi Podvizhnosti. Avtovolnovye Yavleniya v Sokratitel'noi Aktivnosti Plazmodiya Physarum polycephalum* (Mechanochemical Distributed Autooscillations in Cell Motility. Autowave Phenomena in Contractile Activity of *Physarum polycephalum* Plasmodium) (Pushchino: NTsBI Akad. Nauk SSSR, 1987)
86. Kessler D, Nachmias V T, Loewy A G *J. Cell Biol.* **69** 393 (1976)
87. Ueda T, Goetz von Olenhusen K, Wohlfarth-Bottermann K E *Cytobiologie* **18** 76 (1978)
88. Yoshimoto Y, Kamiya N *Cell Struct. Funct.* **9** 135 (1984)
89. Smith D A, Saldana R *Biophys. J.* **61** 368 (1992)
90. Pavlov D A, Potapov M M *Vestn. Mosk. Univ. Vychisl. Matem. Kibern.* **1** 10 (1994)
91. Pavlov D A, Potapov M M *Vest. Mosk. Univ. Vychisl. Matem. Kibern.* **2** 62 (1995)
92. Alt W, Tranquillo R T, in *Proceedings of the 2 European Conference on Mathematics Applied in Biology and Medicine* (Lyon: World Scientific, 1995) (in press)
93. Pavlov D A, Romanovsky Yu M, Teplov V A, in *Biological Motility* (Pushchino: Sci. Centre RAS Press, 1994) p. 258
94. Alt W, in Ref. [93] p. 61
95. Bozhkova V P, Voronov D A, Romanovskii Yu M *Biofizika* **38** 267 (1993)
96. Cheer A, Vincent J P, Nuccitelli R, Oster G *J. Theor. Biol.* **124** 377 (1987)
97. Bozhkova V P, Voronov D A, Romanovsky Yu M, Yagodkin Yu Yu, in Ref. [93] p. 237
98. Evans E, Skalak R *Mechanics and Thermodynamics of Biomembranes* (Boca Raton, FL: CRC Press, 1980)
99. Finer J T, Simmons R M, Spudich J A *Nature (London)* **368** 113 (1994)
100. Teplov V A *Protoplasma Suppl.* **1** 81 (1988)
101. Dembo M, Harlow F *Biophys. J.* **50** 109 (1986)
102. Teplov V A, in Ref. [84] p. 56
103. Priezzhev A V, Tuchin V V, Shubochkin L I *Lazernaya Diagnostika v Biologii i Meditsine* (Laser Diagnostics in Biology and Medicine) (Moscow: Nauka, 1989)
104. Mustacich R V, Ware B R *Phys. Rev. Lett.* **33** 617 (1974)
105. Evdokimov M V, Kolin'ko V G, Poroshina M Yu, Priezzhev A V *Kvant. Elektron.* **12** 2052 (1985)
106. Evdokimov M V, Priezzhev A V, Romanovsky Yu M *Avtometriya* **3** 61 (1982)
107. Johnson R P C, Dumdar G R A, Ross D A, in *Laser Scattering Spectroscopy of Biological Objects* (Eds J Stepanek, P Anzenbacher, B Selacek) (Amsterdam: Elsevier, 1987) p. 531
108. Tanaka I, Nishio I, Peetermans J, Gorti S, in *Laser Applications in Life Sciences* (Eds S A Akhmanov, M Yu Poroshina, N I Koroteev, B Toleutaev) [*Proc. SPIE* **1403** 280 (1990)]
109. Priezzhev A V, Proskurin S G, in *Laser Interferometry IV: Computer-Aided Interferometry* [*Proc. SPIE* **1553** 502 (1992)]
110. Glonty V N, Priezzhev A V, Proskurin S G, Romanovsky Yu M, in *Optics in Medicine, Biology and Environmental Research* (Eds Gert von Bally, Shyam Khanna) (Amsterdam: Elsevier, 1993) p. 161
111. Glonty V N Priezzhev A V, Romanovskii Yu M, in *Lazery v Narodnom Khozyaistve* (Lasers in National Economy) (Moscow: MDNTP, 1988) p. 92
112. Kamiya N *Protoplasmic Streaming* (Vienna: Springer, 1959)
113. Wohlfarth-Bottermann K E *J. Exp. Biol.* **67** 49 (1977)
114. Kolin'ko V G, Arkhangel'skaya T A, Romanovsky Yu M *Studia Biophys.* **106** 215 (1985)
115. Kritskii M S, Chernysheva E K, in *Molekulyarnye Mekhanizmy Biologicheskogo Deistviya Opticheskogo Izlucheniya* (Molecular Mechanisms of Biological Action of Optical Radiation) (Ed. A B Rubin) (Moscow: Nauka, 1988 ) p. 212
116. Schreckenbach T, in *Blue Light Effects in Biological Systems* (Ed. H Senger) (Berlin: Springer, 1984) p. 463
117. Wohlfarth-Bottermann K E *Physarum Newsletter* **22** 1 (1990)
118. Rakoczy L, in *Blue Light Syndrome* (Ed. H Senger) (Berlin: Springer, 1984) p. 570
119. Baranowski Z, Shraiden Z, Wohlfarth-Bottermann K E *Cell Biol. Inter. Rep.* **6** 859 (1982)
120. Wohlfarth-Bottermann K E, Block I *Cell Biol. Inter. Rep.* **5** 365 (1981)
121. Poroshina M Yu, Priezzhev A V, Romanovskii Yu M *Biofizika* **34** 980 (1989)
122. Belenikina N S, Strakhovkaya M G, Freikin G Ya *J. Photochem. Photobiol.* **10** 51 (1991)
123. Pavlov D A, Potapov M M, Romanovsky Yu M, in Ref. [93] p. 72
124. *Blue Light Effects in Biological Systems* (Ed. H Senger) (Berlin: Springer, 1984)
125. Daniel J W *J. Cell Biol.* **87** 23a (1980)
126. Ueda T, Mori Y, Nikagaki I, Kobatake Y *Photochem. Photobiol.* **47** 271 (1988)
127. Ivanitskii G R, Medvinskii A B Tsyganov M A *Usp. Fiz. Nauk* **164** 1041 (1994) [*Phys.-Usp.* **37** 961 (1994)]
128. Tychinsky V, Norina S, Odintsov A, Popp F, Vyshenskaya T, in *Cell and Biotissue Optics* (Ed. V V Tuchin) [*Proc. SPIE* **2110** 129 (1990)]